MIMO Energy Harvesting in Full-Duplex Multi-User Networks

Ho Huu Minh Tam, Hoang Duong Tuan, Ali Arshad Nasir, *Member, IEEE*, Trung Q. Duong, *Senior Member, IEEE*, and H. Vincent Poor, *Fellow, IEEE*

***Abstract*— This paper considers the efficient design of precoding matrices for sum throughput maximization under throughput quality of service (QoS) constraints and energy harvesting (EH) constraints for energy-constrained devices in a full-duplex (FD) multicell multi-user multiple-input-multiple-output network. Both time splitting (TS) and power splitting are considered to ensure practical EH and information decoding. These problems are quite complex due to non-concave objectives and nonconvex constraints. Especially, with TS, which is implementation-wise quite simple, the problem is even more challenging because the time splitting variable is not only coupled with the downlink throughput function but also coupled with the self-interference in the uplink throughput function. New path-following algorithms are developed for their solutions, which require only a single convex quadratic program for each iteration and ensure rapid convergence. Moreover, the FD EH maximization problem under throughput QoS constraints with TS is also considered. The performance of the proposed algorithms is compared with that of the modified problems assuming half-duplex systems. Finally, the merit of the proposed algorithms is demonstrated through extensive simulations.**

***Index Terms*— Full-duplexing transceiver, energy harvesting, information precoder, energy precoder, path-following algorithm, matrix inequality.**

I. Introduction

WIRELESS energy harvesting (EH), in which energy constrained devices scavenge energy from the surrounding radio-frequency (RF) signals, has attracted considerable recent attention from industry and academia [1], [2]. Since the amount of energy opportunistically harvested from ambient/natural energy sources is uncertain and cannot be controlled, base stations (BSs) in small-cell networks can be configured to become dedicated and reliable wireless energy sources [3]. The small cell size not only gives the benefit of efficient resource reuse across a geographic area [4] but also provides an adequate amount of RF energy to battery powered user equipment (UE) for practical applications [1], [2], [5] due to the close BS-UE proximity. In order to transfer both energy and information via the same communication channel, UEs are equipped with both information decoding receivers and energy harvesting receivers. Since the received signal cannot be used for energy harvesting after being decoded, there are two available implementations for wireless energy harvesting and information decoding: (i) receive power splitting (PS), in which a receiver splits the received signal into two streams of different power for decoding information and harvesting energy separately; and (ii) transmit time splitting to enable the receiver to decode information for a portion of a time frame and harvest energy for the rest. Beamforming can be applied to focus the RF signal on the energy harvesting receiver or enhance throughput at the information decoding receiver [5].

Most of the previous works (see e.g. [6], [7] and references therein) focus only on beamforming power optimization subject to information decoding (ID) throughput and EH constraints with PS in multi-input single-output (MISO) networks. The ID throughput constraints are equivalent to signal-to-interference-plus-noise ratio (SINR) constraints, which are indefinite quadratic in the beamforming vectors. The harvested energy constraints are also indefinite quadratic constraints. Thus, [6] and [7] used semi-definite relaxation (SDR) to relax such indefinite quadratic optimization problems to semi-definite programs (SDPs) by dropping the matrix rank-one constraints on the outer products of the beamforming vectors. The variable dimension of SDP is explosively large, and the beamforming vectors that are recovered based on the matrix solution of SDR perform poorly [8]. Moreover, SDR cannot be applied to throughput or EH maximization as the problems resulting from SDR are still nonconvex. Only recently has there been an effective development to address these problems in [9] and [10].

Considering multiple-input multiple-output (MIMO) interference channels, information throughput and harvested energy, i.e., the rate-energy (R-E) trade-off, was investigated in [11] and [12], assuming that any UE acts either as an ID receiver or an EH receiver. In the situation in which UEs can operate both as ID receivers and EH receivers (namely co-

Manuscript received September 13, 2016; revised November 30, 2016 and February 21, 2017; accepted February 21, 2017. Date of publication March 17, 2017; date of current version May 8, 2017. This work was supported in part by the Australian Research Councils Discovery Projects under Project DP130104617, in part by the U.K. Royal Academy of Engineering Research Fellowship under Grant RF1415/14/22, in part by the U.K. Engineering and Physical Sciences Research Council under Grant EP/P019374/1, in part by the U.S. National Science Foundation under Grant CNS-1456793 and Grant ECCS-1647198, and in part by the King Fahd University of Petroleum and Minerals under Start-up Research Project under Grant SR161003. The associate editor coordinating the review of this paper and approving it for publication was P. Salvo Rossi.

H. H. M. Tam and H. D. Tuan are with the Faculty of Engineering and Information Technology, University of Technology Sydney, Broadway, NSW 2007, Australia (e-mail: huuminhtam.ho@student.uts.edu.au; tuan.hoang@uts.edu.au).

A. A. Nasir is with the Department of Electrical Engineering, King Fahd University of Petroleum and Minerals, Dhahran 31261, Saudi Arabia (e-mail: anasir@kfupm.edu.sa).

T. Q. Duong is with Queen's University Belfast, Belfast BT7 1NN, U.K. (e-mail: trung.q.duong@qub.ac.uk).

H. V. Poor is with the Department of Electrical Engineering, Princeton University, Princeton, NJ 08544 USA (e-mail: poor@princeton.edu).

Color versions of one or more of the figures in this paper are available online at http://ieeexplore.ieee.org.

Digital Object Identifier 10.1109/TWC.2017.2679055

located cases), the R-E region of the point-to-point MIMO channel was studied in [13]. Note that in MIMO networks, the information throughput function involves the determinant of a matrix and can no longer be expressed in the form of SINR. Consequently, the throughput constraints make precoder design very challenging in this case. References [14] and [15] used zero-forcing or interference-alignment to cancel all interference, making the throughput functions concave in the signal covariance. The covariance optimization becomes convex but it is still computationally difficult with no available algorithm of polynomial complexity. Moreover, there is no known method to recover the precoder matrices from the signal covariance. Recently, the MIMO throughput function optimization has been successfully addressed for a non-EH system in our previous work via successive convex quadratic programming [16]. The result of [16] can be adapted to MIMO networks that employ PS EH. However, there is very little research on systems employing TS in MIMO networks. Though TS-based systems are easier to implement, the related formulated problem is quite complex because the throughput function in this case is coupled with the TS variable that defines the portions of the time slot dedicated to EH and ID. This renders the aforementioned precoder design [14]–[16] for PS inapplicable. To the best of our knowledge, both the throughput maximization problem and the harvested energy maximization problem with TS are still open.

All aforementioned works assume that UEs harvest energy arriving from the BSs' downlink (DL) transmission. In reality, UEs can also opportunistically harvest energy from the other UEs' signals during their uplink (UL) transmissions. Furthermore, by allowing the BSs to simultaneously transmit and receive information, both the spectral efficiency and the amount of transferred energy will be improved. With the recent advances in antenna design and RF circuits in reducing self-interference (SI) [17]–[20], which is the interference from a BS's DL transmitter to its UL receiver, full duplex (FD) technology has recently been proposed as one of the key transceiving techniques for fifth generation (5G) networks [20]–[24]. In this paper, we are interested in a network in which each FD multi-antenna BS simultaneously serves a group of UL UEs (ULUs) and a group of DL UEs (DLUs). At the same time, the BS also transfers energy to DLUs via TS or PS. FD transmission introduces even more interference into the network by adding not only SI but also the interference from ULUs toward DLUs and the interference from DL transmissions of other BSs. Consequently, the UL and DL precoders are coupled in both DL and UL throughput functions, which makes the optimization problems for UL transmission and DL transmission inseparable.

In the literature, [14], [25], and [26] proposed covariance matrix design in (non-EH) FD multiuser-MIMO (MU-MIMO) networks using D.C. (difference of convex functions) iterations [27], which are still very computationally demanding as they require log-determinant function optimizations as mentioned above. Our previous work [16] has recently proposed a framework to directly find the optimal precoding matrices for the sum throughput maximization under throughput constraints in FD MU-MIMO multi-cell networks, which requires only a convex quadratic program of moderate size at each iteration and thus is very computationally efficient.

In this paper, we propose the design of efficient precoding matrices for the network sum throughput maximization under QoS constraints in terms of MIMO throughput constraints and EH constraints in an FD EH-enabled multicell MU-MIMO network. Both PS and TS are considered for the precoder designs, and both problems are quite challenging computationally due to their nonconcave objective functions and nonconvex constraints. However, we will see that the PS problem can be efficiently addressed by adapting the algorithm of [16]. On the other hand, the TS problem is much more challenging because the TS variable is not only coupled with the DL throughput function but is also coupled with the SI in the UL throughput function. It is nontrivial to extend [16] to solve the TS problem. Toward this end, we develop a new inner approximation of the original problem and solve it by a path-following algorithm. Finally, we also consider the FD EH maximization problem with throughput QoS constraints with TS. This problem also has a nonconvex objective function and nonconvex constraints and will be addressed by applying an approach similar to that proposed for the TS problem.

The rest of this paper is organized as follows: Section II presents the system model and the SCP algorithm for the PS problem. The main contributions of the paper are in Section III and Section IV, which develop algorithms for the TS problem and FD EH maximization problem. Section V evaluates the performance of our devised solutions via numerical examples. Finally, Section VI concludes the paper.

Notation: All variables are boldfaced. I_n denotes the identity matrix of size $n \times n$. The notation $(\cdot)^H$ stands for the Hermitian transpose. $|A|$ denotes the determinant of a square matrix A and $\langle A \rangle$ denotes the trace of a matrix A. $(A)^2$ denotes the Hermitian symmetric positive definite matrix AA^H. The inner product $\langle X, Y \rangle$ is defined as $\langle X^H Y \rangle$ and therefore the Frobenius squared norm of a matrix X is $||X||^2 = \langle (X)^2 \rangle$. The notation $A \succeq B$ ($A \succ B$, respectively) means that $A - B$ is a positive semidefinite (definite, respectively) matrix. $\mathbb{E}[\cdot]$ denotes the expectation and $\Re\{\cdot\}$ denotes the real part of a complex number.

The following concept of function approximation [28] plays an important role in our development.

Definition: A function $\tilde{f}$ is called a (global) minorant of a function f at a point $\bar{x}$ in the definition domain $\mathrm{dom}(f)$ of f if $\tilde{f}(\bar{x}) = f(\bar{x})$ and $f(\mathbf{x}) \geq \tilde{f}(\mathbf{x})\ \forall\ \mathbf{x} \in \mathrm{dom}(f)$.

The following result [16] is used.

Theorem 1: Consider the function $f(\mathbf{V}, \mathbf{Y}) = \ln|I_n + \mathbf{V}^H \mathbf{Y}^{-1} \mathbf{V}|$ in the matrix variable $\mathbf{V} \in \mathbb{C}^{n \times m}$ and positive definite matrix variable $\mathbf{Y} \in \mathbb{C}^{m \times m}$. The following quadratic function is its minorant at $(\bar{V}, \bar{Y})$:

$$\tilde{f}(\mathbf{V}, \mathbf{Y}) = a + 2\Re\{\langle \mathcal{A}, \mathbf{V} \rangle\} - \langle \mathcal{B}, \mathbf{V}\mathbf{V}^H + \mathbf{Y} \rangle,$$

where $0 > a \triangleq f(\bar{V}, \bar{Y}) - \langle \bar{V}^H \bar{Y}^{-1} \bar{V} \rangle$, $\mathcal{A} = \bar{Y}^{-1} \bar{V}$ and $0 \preceq \mathcal{B} = \bar{Y}^{-1} - (\bar{Y} + \bar{V}\bar{V}^H)^{-1}$.

II. EH-Enabled FD MU-MIMO Networks

We consider an MU-MIMO EH-enable network consisting of I cells. In cell $i \in \{1, \ldots, I\}$, a group of D DLUs in the DL

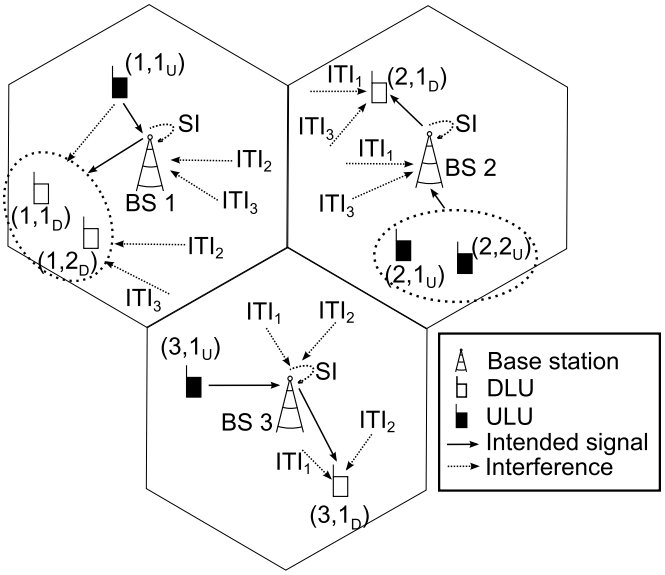

Fig. 1. Interference scenario in an FD multicell network, where SI denotes the self-interference and ITI_i denotes the interference from the BS and ULUs of cell i.

channel and a group of U ULUs in the UL channel are served by a BS i as illustrated in Fig. 1. Each BS operates in the FD mode and is equipped with $N \triangleq N_1 + N_2$ antennas, where N_1 antennas are used to transmit and the remaining N_2 antennas to receive signals. In cell i, DLU (i, j_{D}) and ULU (i, j_{U}) operate in the HD mode and each is equipped with N_r antennas. In the DL, let $s_{i,j_{\mathsf{D}}} \in \mathbb{C}^{d_1}$ be the symbol intended for DLU (i, j_{D}) where $\mathbb{E}\left[s_{i,j_{\mathsf{D}}}(s_{i,j_{\mathsf{D}}})^H\right] = I_{d_1}$, d_1 is the number of concurrent data streams and $d_1 \leq \min\{N_1, N_r\}$. The vector of symbols $s_{i,j_{\mathsf{D}}}$ is precoded and transmitted to DLU (i, j_{D}) through the precoding matrix $\mathbf{V}_{i,j_{\mathsf{D}}} \in \mathbb{C}^{N_1 \times d_1}$. Analogously, in the UL, $s_{i,j_{\mathsf{U}}} \in \mathbb{C}^{d_2}$ is the information symbols sent by ULU (i, j_{U}) and is precoded by the precoding matrix $\mathbf{V}_{i,j_{\mathsf{U}}} \in \mathbb{C}^{N_r \times d_2}$, where $\mathbb{E}\left[s_{i,j_{\mathsf{U}}}(s_{i,j_{\mathsf{U}}})^H\right] = I_{d_2}$, d_2 is the number of concurrent data streams and $d_2 \leq \min\{N_2, N_r\}$. For notational convenience, let us define

$$\begin{aligned}
&\mathcal{I} \triangleq \{1, 2, \ldots, I\}; \quad \mathcal{D} \triangleq \{1_{\mathsf{D}}, 2_{\mathsf{D}}, \ldots, D_{\mathsf{D}}\};\\
&\mathcal{U} \triangleq \{1_{\mathsf{U}}, 2_{\mathsf{U}}, \ldots, U_{\mathsf{U}}\}; \mathcal{S}_1 \triangleq \mathcal{I} \times \mathcal{D}; \quad \mathcal{S}_2 \triangleq \mathcal{I} \times \mathcal{U};\\
&\mathbf{V}_{\mathsf{D}} = [\mathbf{V}_{i,j_{\mathsf{D}}}]_{(i,j_{\mathsf{D}})\in\mathcal{S}_1}; \mathbf{V}_{\mathsf{U}} = [\mathbf{V}_{i,j_{\mathsf{U}}}]_{(i,j_{\mathsf{U}})\in\mathcal{S}_2};\\
&\mathbf{V} \triangleq [\mathbf{V}_{\mathsf{D}}\ \mathbf{V}_{\mathsf{U}}].
\end{aligned}$$

In the DL channel, the received signal at DLU (i, j_{D}) can be expressed as

$$\begin{aligned}
y_{i,j_{\mathsf{D}}} \triangleq\ & \underbrace{H_{i,i,j_{\mathsf{D}}}\mathbf{V}_{i,j_{\mathsf{D}}}s_{i,j_{\mathsf{D}}}}_{\text{desired signal}}\\
&+ \underbrace{\sum_{(m,\ell_{\mathsf{D}})\in\mathcal{S}_1\setminus(i,j_{\mathsf{D}})} H_{m,i,j_{\mathsf{D}}}\mathbf{V}_{m,\ell_{\mathsf{D}}}s_{m,\ell_{\mathsf{D}}}}_{\text{DL interference}}\\
&+ \underbrace{\sum_{\ell_{\mathsf{U}}\in\mathcal{U}} H_{i,j_{\mathsf{D}},\ell_{\mathsf{U}}}\mathbf{V}_{i,\ell_{\mathsf{U}}}s_{i,\ell_{\mathsf{U}}}}_{\text{UL intracell interference}} + n_{i,j_{\mathsf{D}}}, \qquad (1)
\end{aligned}$$

where $H_{m,i,j_{\mathsf{D}}} \in \mathbb{C}^{N_r \times N_1}$ and $H_{i,j_{\mathsf{D}},\ell_{\mathsf{U}}} \in \mathbb{C}^{N_r \times N_r}$ are the channel matrices from BS m to DLU (i, j_{D}) and from ULU (i, ℓ_{U}) to DLU (i, j_{D}), respectively. Also, $n_{i,j_{\mathsf{D}}}$ is the additive white circularly symmetric complex Gaussian noise with variance σ_{D}^2. In this work, the UL intercell interference is neglected since it is very small compared to the DL intercell interference due to the much smaller transmit power of ULUs. Nevertheless, it can be incorporated easily into our formulation.

Assuming that DLUs are equipped with devices for both ID and EH, the power splitting technique is applied at each DLU to simultaneously conduct information decoding and energy harvesting. The power splitter divides the received signal $y_{i,j_{\mathsf{D}}}$ into two parts in the proportion of $\boldsymbol{\alpha}_{i,j_{\mathsf{D}}} : (1-\boldsymbol{\alpha}_{i,j_{\mathsf{D}}})$ where $\boldsymbol{\alpha}_{i,j_{\mathsf{D}}} \in (0, 1)$ is termed the PS ratio for DLU (i, j_{D}). In particular, the signal split to the ID receiver of DLU (i, j_{D}) is given by

$$\sqrt{\boldsymbol{\alpha}_{i,j_{\mathsf{D}}}}y_{i,j_{\mathsf{D}}} + z^c_{i,j_{\mathsf{D}}}, \qquad (2)$$

where each r-th element of $z^c_{i,j_{\mathsf{D}}}$ $(\mathrm{E}\{|z^c_{i,j_{\mathsf{D}},r}|^2\} = \sigma_c^2$, $r = 1, ..., N_r)$ is additional noise introduced by the ID receiver circuity. An EH receiver processes the second part of the split signal $\sqrt{1-\boldsymbol{\alpha}_{i,j_{\mathsf{D}}}}y_{i,j_{\mathsf{D}}}$ for the harvested energy

$$\sqrt{\zeta_{i,j_{\mathsf{D}}}(1-\boldsymbol{\alpha}_{i,j_{\mathsf{D}}})}y_{i,j_{\mathsf{D}}},$$

where $\zeta_{i,j_{\mathsf{D}}} \in (0.4, 0.6)$ is the efficiency of energy conversion.

It follows from the receive equation (1) and the split equation (2) that the downlink information throughput at DLU (i, j_{D}) is

$$\begin{aligned}
&f_{i,j_{\mathsf{D}}}(\mathbf{V}_{\mathsf{D}}, \mathbf{V}_{\mathsf{U}}, \boldsymbol{\alpha}_{i,j_{\mathsf{D}}})\\
&\quad\triangleq \ln\left|I_{N_r} + (\mathcal{L}_{i,j_{\mathsf{D}}}(\mathbf{V}_{i,j_{\mathsf{D}}}))^2\Psi^{-1}_{i,j_{\mathsf{D}}}(\mathbf{V}_{\mathsf{D}}, \mathbf{V}_{\mathsf{U}}, \boldsymbol{\alpha}_{i,j_{\mathsf{D}}})\right|, \qquad (3)
\end{aligned}$$

where $\mathcal{L}_{i,j_{\mathsf{D}}}(\mathbf{V}_{i,j_{\mathsf{D}}}) \triangleq H_{i,i,j_{\mathsf{D}}}\mathbf{V}_{i,j_{\mathsf{D}}}$ and

$$\Psi_{i,j_{\mathsf{D}}}(\mathbf{V}_{\mathsf{D}}, \mathbf{V}_{\mathsf{U}}, \boldsymbol{\alpha}_{i,j_{\mathsf{D}}}) \triangleq \bar{\Psi}_{i,j_{\mathsf{D}}}(\mathbf{V}_{\mathsf{D}}, \mathbf{V}_{\mathsf{U}}) + (\sigma_c^2/\boldsymbol{\alpha}_{i,j_{\mathsf{D}}})I_{N_r} \qquad (4)$$

with the *downlink interference covariance mapping*

$$\begin{aligned}
\bar{\Psi}_{i,j_{\mathsf{D}}}(\mathbf{V}_{\mathsf{D}}, \mathbf{V}_{\mathsf{U}}) \triangleq\ & \sum_{(m,\ell_{\mathsf{D}})\in\mathcal{S}_1\setminus(i,j_{\mathsf{D}})} (H_{m,i,j_{\mathsf{D}}}\mathbf{V}_{m,\ell_{\mathsf{D}}})^2\\
&+ \sum_{\ell_{\mathsf{U}}\in\mathcal{U}} (H_{i,j_{\mathsf{D}},\ell_{\mathsf{U}}}\mathbf{V}_{i,\ell_{\mathsf{U}}})^2 + \sigma_{\mathsf{D}}I_{N_r}. \qquad (5)
\end{aligned}$$

The harvested energy at UE (i, j_{D}) is

$$E_{i,j_{\mathsf{D}}}(\mathbf{V}_{\mathsf{D}}, \mathbf{V}_{\mathsf{U}}, \boldsymbol{\alpha}_{i,j_{\mathsf{D}}}) = \zeta_{i,j_{\mathsf{D}}}(1-\boldsymbol{\alpha}_{i,j_{\mathsf{D}}})\langle\Phi_{i,j_{\mathsf{D}}}(\mathbf{V}_{\mathsf{D}}, \mathbf{V}_{\mathsf{U}})\rangle, \qquad (6)$$

with the *downlink signal covariance mapping*

$$\begin{aligned}
\Phi_{i,j_{\mathsf{D}}}(\mathbf{V}_{\mathsf{D}}, \mathbf{V}_{\mathsf{U}}) \triangleq\ & \sum_{(m,\ell_{\mathsf{D}})\in\mathcal{S}_1} (H_{m,i,j_{\mathsf{D}}}\mathbf{V}_{m,\ell_{\mathsf{D}}})^2\\
&+ \sum_{\ell_{\mathsf{U}}\in\mathcal{U}} (H_{i,j_{\mathsf{D}},\ell_{\mathsf{U}}}\mathbf{V}_{i,\ell_{\mathsf{U}}})^2 + \sigma_{\mathsf{D}}^2 I_{N_r}. \qquad (7)
\end{aligned}$$

In the UL channel, the received signal at BS i can be written as

$$y_i \triangleq \underbrace{\sum_{\ell_{\mathsf{U}}\in\mathcal{U}} H_{i,\ell_{\mathsf{U}},i}\mathbf{V}_{i,\ell_{\mathsf{U}}}s_{i,\ell_{\mathsf{U}}}}_{\text{desired signal}} + \underbrace{\sum_{m\in I\setminus\{i\}}\sum_{\ell_{\mathsf{U}}\in\mathcal{U}} H_{m,\ell_{\mathsf{U}},i}\mathbf{V}_{m,\ell_{\mathsf{U}}}s_{m,\ell_{\mathsf{U}}}}_{\text{UL interference}} + \underbrace{\sum_{m\in I\setminus\{i\}} H^{\mathcal{B}}_{m,i}\sum_{j_{\mathsf{D}}\in\mathcal{D}}\mathbf{V}_{m,j_{\mathsf{D}}}s_{m,j_{\mathsf{D}}}}_{\text{DL intercell interference}} + \underbrace{n_i^{SI}}_{\text{residual SI}} + n_i, \quad (8)$$

where $H_{m,\ell_{\mathsf{U}},i} \in \mathbb{C}^{N_2\times N_r}$ and $H^{\mathcal{B}}_{m,i} \in \mathbb{C}^{N_2\times N_1}$ are channel matrices from ULU (m,ℓ_{U}) to BS i and from BS m to BS i, respectively; and n_i is additive white circularly symmetric complex Gaussian noise with variance σ^2_{U}; and n_i^{SI} is the residual SI (after self-interference cancellation) at BS i which depends on the transmit power of BS i. Specifically, n_i^{SI} is modelled as additive white circularly symmetric complex Gaussian noise with variance $\sigma^2_{SI}\sum_{\ell_{\mathsf{D}}\in\mathcal{D}}||\mathbf{V}_{i,\ell_{\mathsf{D}}}||^2$ [29], where the SI level σ^2_{SI} is the ratio of the average SI powers after and before the SI cancellation process.

Following [14], [16], and [26], the minimum mean square error - successive interference cancellation (MMSE-SIC) decoder is applied at the BSs. Therefore, the achievable uplink throughput at BS i is given as [30]

$$f_i(\mathbf{V}_{\mathsf{D}},\mathbf{V}_{\mathsf{U}}) \triangleq \ln\left|I_{N_2} + (\mathcal{L}_i(\mathbf{V}_{\mathsf{U}_i}))^2\Psi_i^{-1}(\mathbf{V}_{\mathsf{D}},\mathbf{V}_{\mathsf{U}})\right|, \quad (9)$$

where $\mathbf{V}_{\mathsf{U}_i} \triangleq [\mathbf{V}_{i,\ell_{\mathsf{U}}}]_{\ell_{\mathsf{U}}\in\mathcal{U}}$ and $\mathcal{L}_i(\mathbf{V}_{\mathsf{U}i}) \triangleq \left[H_{i,1_{\mathsf{U}},i}\mathbf{V}_{i,1_{\mathsf{U}}}, H_{i,2_{\mathsf{U}},i}\mathbf{V}_{i,2_{\mathsf{U}}},\ldots,H_{i,U_{\mathsf{U}},i}\mathbf{V}_{i,U_{\mathsf{U}}}\right]$, which means that $(\mathcal{L}_i(\mathbf{V}_{\mathsf{U}i}))^2 = \sum_{\ell=1}^{U}(H_{i,\ell_{\mathsf{U}},i}\mathbf{V}_{i,\ell_{\mathsf{U}}})^2$, and

$$\Psi_i(\mathbf{V}_{\mathsf{D}},\mathbf{V}_{\mathsf{U}}) \triangleq \bar{\Psi}_i^{U}(\mathbf{V}_{\mathsf{U}}) + \bar{\Psi}_i^{SI}(\mathbf{V}_{\mathsf{D}}) \quad (10)$$

with *uplink interference covariance mapping*

$$\bar{\Psi}_i^{U}(\mathbf{V}_{\mathsf{U}}) \triangleq \sum_{m\in I\setminus\{i\}}\sum_{\ell_{\mathsf{U}}\in\mathcal{U}}(H_{m,\ell_{\mathsf{U}},i}\mathbf{V}_{m,\ell_{\mathsf{U}}})^2 + \sum_{m\in I\setminus\{i\}} H^{\mathcal{B}}_{m,i}\left(\sum_{j_{\mathsf{D}}\in\mathcal{D}}(\mathbf{V}_{m,j_{\mathsf{D}}})^2\right)(H^{\mathcal{B}}_{m,i})^H + \sigma^2_{\mathsf{U}}I_{N_2} \quad (11)$$

and *SI covariance mapping*

$$\bar{\Psi}_i^{SI}(\mathbf{V}_{\mathsf{D}}) \triangleq \sigma^2_{SI}\sum_{\ell_{\mathsf{D}}\in\mathcal{D}}||\mathbf{V}_{i,\ell_{\mathsf{D}}}||^2 I_{N_2}. \quad (12)$$

We consider the design problem

$$\max_{\mathbf{V}_{\mathsf{D}},\mathbf{V}_{\mathsf{U}},\boldsymbol{\alpha}} \mathcal{P}_1(\mathbf{V}_{\mathsf{D}},\mathbf{V}_{\mathsf{U}},\boldsymbol{\alpha}) \triangleq \sum_{i\in I} f_i(\mathbf{V}_{\mathsf{D}},\mathbf{V}_{\mathsf{U}}) + \sum_{(i,j_{\mathsf{D}})\in\mathcal{S}_1} f_{i,j_{\mathsf{D}}}(\mathbf{V}_{\mathsf{D}},\mathbf{V}_{\mathsf{U}},\boldsymbol{\alpha}_{i,j_{\mathsf{D}}}) \quad \text{s.t.} \quad (13a)$$

$$0 < \boldsymbol{\alpha}_{i,j_{\mathsf{D}}} < 1, (i,j_{\mathsf{D}}) \in \mathcal{S}_1, \quad (13b)$$

$$\sum_{(i,j_{\mathsf{D}})\in\mathcal{S}_1}||\mathbf{V}_{i,j_{\mathsf{D}}}||^2 + \sum_{(i,j_{\mathsf{U}})\in\mathcal{S}_2}||\mathbf{V}_{i,j_{\mathsf{U}}}||^2 \le P, \quad (13c)$$

$$\sum_{j_{\mathsf{D}}\in\mathcal{D}}||\mathbf{V}_{i,j_{\mathsf{D}}}||^2 \le P_i, \quad \forall i \in I, \quad (13d)$$

$$||\mathbf{V}_{i,j_{\mathsf{U}}}||^2 \le P_{i,j_{\mathsf{U}}}, \quad \forall (i,j_{\mathsf{U}}) \in \mathcal{S}_2, \quad (13e)$$

$$\langle\Phi_{i,j_{\mathsf{D}}}(\mathbf{V}_{\mathsf{D}},\mathbf{V}_{\mathsf{U}})\rangle \ge e^{\min}_{i,j_{\mathsf{D}}}/\zeta_{i,j_{\mathsf{D}}}(1-\boldsymbol{\alpha}_{i,j_{\mathsf{D}}}), \forall (i,j_{\mathsf{D}}) \in \mathcal{S}_1, \quad (13f)$$

$$f_i(\mathbf{V}_{\mathsf{D}},\mathbf{V}_{\mathsf{U}}) \ge r_i^{\mathsf{U},\min}, \quad \forall i \in I \quad (13g)$$

$$f_{i,j_{\mathsf{D}}}(\mathbf{V}_{\mathsf{D}},\mathbf{V}_{\mathsf{U}},\boldsymbol{\alpha}_{i,j_{\mathsf{D}}}) \ge r_{i,j_{\mathsf{D}}}^{\mathsf{D},\min}, \quad \forall (i,j_{\mathsf{D}}) \in \mathcal{S}_1. \quad (13h)$$

In the formulation (13), all channel matrices in the downlink equation (1) and uplink (8) are assumed to be known by using channel reciprocity, feedback and learning mechanisms (see e.g. [31]). The convex constraints (13d) and (13e) specify the maximum transmit power available at the BSs and the ULUs whereas (13c) limits the total transmit power of the whole network. The nonconvex constraints (13f), (13g) and (13h) represent QoS guarantees, where $e^{\min}_{i,j_{\mathsf{D}}}$, $r_i^{\mathsf{U},\min}$ and $r_{i,j_{\mathsf{D}}}^{\mathsf{D},\min}$ are respectively the minimum harvested energy required by DLU (i,j_{D}), the minimum data throughput required by BS i, and the minimum data throughput required by DLU (i,j_{D}). In comparison to [16] for FD non-EH-enabled networks, the UL throughput function $f_i(\mathbf{V}_{\mathsf{D}},\mathbf{V}_{\mathsf{U}})$ in (9) is the same, where the DL throughput function $f_{i,j_{\mathsf{D}}}(\mathbf{V}_{\mathsf{D}},\mathbf{V}_{\mathsf{U}},\boldsymbol{\alpha}_{i,j_{\mathsf{D}}})$ is now additionally dependent on the PS ratio $\boldsymbol{\alpha}_{i,j_{\mathsf{D}}}$, is decoupled in (5) and thus does not add more difficulty as we will show now. We also show that the nonconvex EH constraints (13f) can easily be innerly approximated.

On defining

$$\mathcal{M}_{i,j_{\mathsf{D}}}(\mathbf{V}_{\mathsf{D}},\mathbf{V}_{\mathsf{U}},\boldsymbol{\alpha}_{i,j_{\mathsf{D}}}) \triangleq (\mathcal{L}_{i,j_{\mathsf{D}}}(\mathbf{V}_{i,j_{\mathsf{D}}}))^2 + \Psi_{i,j_{\mathsf{D}}}(\mathbf{V}_{\mathsf{D}},\mathbf{V}_{\mathsf{U}},\boldsymbol{\alpha}_{i,j_{\mathsf{D}}}) \quad (14)$$

$$\succeq \Psi_{i,j_{\mathsf{D}}}(\mathbf{V}_{\mathsf{D}},\mathbf{V}_{\mathsf{U}},\boldsymbol{\alpha}_{i,j_{\mathsf{D}}}), \quad (15)$$

$$\mathcal{M}_i(\mathbf{V}_{\mathsf{D}},\mathbf{V}_{\mathsf{U}}) \triangleq (\mathcal{L}_i(\mathbf{V}_{\mathsf{U}i}))^2 + \Psi_i(\mathbf{V}_{\mathsf{D}},\mathbf{V}_{\mathsf{U}}) \quad (16)$$

$$\succeq \Psi_i(\mathbf{V}_{\mathsf{D}},\mathbf{V}_{\mathsf{U}}), \quad (17)$$

and applying Theorem 1 as in [16], we obtain the following concave quadratic minorants of the throughput functions $f_{i,j_{\mathsf{D}}}(\mathbf{V}_{\mathsf{D}},\mathbf{V}_{\mathsf{U}},\boldsymbol{\alpha}_{i,j_{\mathsf{D}}})$ and $f_i(\mathbf{V}_{\mathsf{D}}^{(\kappa)},\mathbf{V}_{\mathsf{U}}^{(\kappa)})$ at $(V_{\mathsf{D}}^{(\kappa)}, V_{\mathsf{U}}^{(\kappa)}, \alpha^{(\kappa)}) \triangleq ([V^{(\kappa)}_{i,j_{\mathsf{D}}}]_{(i,j_{\mathsf{D}})\in\mathcal{S}_1}, [V^{(\kappa)}_{i,\ell_{\mathsf{U}}}]_{(i,\ell_{\mathsf{U}})\in\mathcal{S}_2}, [\alpha^{(\kappa)}_{i,j_{\mathsf{D}}}]_{(i,j_{\mathsf{D}})\in\mathcal{S}_1})$:

$$\Theta^{(\kappa)}_{i,j_{\mathsf{D}}}(\mathbf{V}_{\mathsf{D}},\mathbf{V}_{\mathsf{U}},\boldsymbol{\alpha}_{i,j_{\mathsf{D}}}) \triangleq a^{(\kappa)}_{i,j_{\mathsf{D}}} + 2\Re\left\{\langle\mathcal{A}^{(\kappa)}_{i,j_{\mathsf{D}}},\mathcal{L}_{i,j_{\mathsf{D}}}(\mathbf{V}_{i,j_{\mathsf{D}}})\rangle\right\} - \langle\mathcal{B}^{(\kappa)}_{i,j_{\mathsf{D}}},\mathcal{M}_{i,j_{\mathsf{D}}}(\mathbf{V}_{\mathsf{D}},\mathbf{V}_{\mathsf{U}},\boldsymbol{\alpha}_{i,j_{\mathsf{D}}})\rangle \quad (18)$$

and

$$\Theta_i^{(\kappa)}(\mathbf{V}_\mathsf{D}, \mathbf{V}_\mathsf{U}) \triangleq a_i^{(\kappa)} + 2\Re\left\{\langle \mathcal{A}_i^{(\kappa)}, \mathcal{L}_i(\mathbf{V}_{\mathsf{U}_i})\rangle\right\} - \langle \mathcal{B}_i^{(\kappa)}, \mathcal{M}_i(\mathbf{V}_\mathsf{D}, \mathbf{V}_\mathsf{U})\rangle, \tag{19}$$

where

$$\begin{aligned} 0 > a_{i,j_\mathsf{D}}^{(\kappa)} &\triangleq f_{i,j_\mathsf{D}}(V_\mathsf{D}^{(\kappa)}, V_\mathsf{U}^{(\kappa)}, \alpha_{i,j_\mathsf{D}}^{(\kappa)}) \\ &\quad - \Re\left\{\langle \Psi_{i,j_\mathsf{D}}^{-1}(V_\mathsf{D}^{(\kappa)}, V_\mathsf{U}^{(\kappa)}) \mathcal{L}_{i,j_\mathsf{D}}(V_{i,j_\mathsf{D}}^{(\kappa)}), \right. \\ &\qquad \left. \mathcal{L}_{i,j_\mathsf{D}}(V_{i,j_\mathsf{D}}^{(\kappa)})\rangle\right\}, \\ \mathcal{A}_{i,j_\mathsf{D}}^{(\kappa)} &= \Psi_{i,j_\mathsf{D}}^{-1}(V_\mathsf{D}^{(\kappa)}, V_\mathsf{U}^{(\kappa)}, \alpha_{i,j_\mathsf{D}}^{(\kappa)}) \mathcal{L}_{i,j_\mathsf{D}}(V_{i,j_\mathsf{D}}^{(\kappa)}), \\ 0 \preceq \mathcal{B}_{i,j_\mathsf{D}}^{(\kappa)} &= \Psi_{i,j_\mathsf{D}}^{-1}(V_\mathsf{D}^{(\kappa)}, V_\mathsf{U}^{(\kappa)}, \alpha_{i,j_\mathsf{D}}^{(\kappa)}) \\ &\quad - \mathcal{M}_{i,j_\mathsf{D}}^{-1}(V_\mathsf{D}^{(\kappa)}, V_\mathsf{U}^{(\kappa)}, \alpha_{i,j_\mathsf{D}}^{(\kappa)}), \end{aligned} \tag{20}$$

and

$$\begin{aligned} 0 > a_i^{(\kappa)} &= f_i(V_\mathsf{D}^{(\kappa)}, V_\mathsf{U}^{(\kappa)}) \\ &\quad - \Re\left\{\langle \Psi_i^{-1}(V_\mathsf{D}^{(\kappa)}, V_\mathsf{U}^{(\kappa)}) \mathcal{L}_i(V_i^{(\kappa)}), \mathcal{L}_i(V_i^{(\kappa)})\rangle\right\}, \\ \mathcal{A}_i^{(\kappa)} &= \Psi_i^{-1}(V_\mathsf{D}^{(\kappa)}, V_\mathsf{U}^{(\kappa)}) \mathcal{L}_i(V_{\mathsf{U}_i}^{(\kappa)}), \\ 0 \preceq \mathcal{B}_i^{(\kappa)} &= \Psi_i^{-1}(V_\mathsf{D}^{(\kappa)}, V_\mathsf{U}^{(\kappa)}) \\ &\quad - \mathcal{M}_i^{-1}(V_\mathsf{D}^{(\kappa)}, V_\mathsf{U}^{(\kappa)}). \end{aligned} \tag{21}$$

To handle the nonconvex EH constraints (13f), we define an affine function $\phi_{i,j_\mathsf{D}}^{(\kappa)}(\mathbf{V}_\mathsf{D}, \mathbf{V}_\mathsf{U})$ as the first-order approximation of the convex function $\langle \Phi_{i,j_\mathsf{D}}(\mathbf{V}_\mathsf{D}, \mathbf{V}_\mathsf{U})\rangle$ at $(V_\mathsf{D}^{(\kappa)}, V_\mathsf{U}^{(\kappa)})$:

$$\begin{aligned} \phi_{i,j_\mathsf{D}}^{(\kappa)}(\mathbf{V}_\mathsf{D}, \mathbf{V}_\mathsf{U}) &\triangleq -\langle \Phi_{i,j_\mathsf{D}}(V_\mathsf{D}^{(\kappa)}, V_\mathsf{U}^{(\kappa)})\rangle \\ &\quad + 2\Re\{\sum_{(m,\ell_\mathsf{D})\in\mathcal{S}_1} \langle H_{m,i,j_\mathsf{D}} V_{m,\ell_\mathsf{D}}^{(\kappa)} \mathbf{V}_{m,\ell_\mathsf{D}} H_{m,i,j_\mathsf{D}}^H\rangle\} \\ &\quad + 2\Re\{\sum_{\ell_\mathsf{U}\in\mathcal{U}} \langle H_{i,i_\mathsf{D},\ell_\mathsf{U}} V_{i,\ell_\mathsf{U}}^{(\kappa)} \mathbf{V}_{i,\ell_\mathsf{U}}^H H_{i,i_\mathsf{D},\ell_\mathsf{U}}^H\rangle\} \\ &\quad + 2\sigma_\mathsf{D}^2 N_r, \end{aligned} \tag{22}$$

which is an minorant of $\langle \Phi_{i,j_\mathsf{D}}(\mathbf{V}_\mathsf{D}, \mathbf{V}_\mathsf{U})\rangle$ at $(V_\mathsf{D}^{(\kappa)}, V_\mathsf{U}^{(\kappa)})$ [28].

We now address the nonconvex problem (13) by successively solving its following inner approximation:

$$\max_{\mathbf{V}_\mathsf{D}, \mathbf{V}_\mathsf{U}, \boldsymbol{\alpha}} \ \mathcal{P}_1^{(\kappa)}(\mathbf{V}_\mathsf{D}, \mathbf{V}_\mathsf{U}, \boldsymbol{\alpha}) \triangleq \sum_{i\in I} \Theta_i^{(\kappa)}(\mathbf{V}_\mathsf{D}, \mathbf{V}_\mathsf{U}) + \sum_{(i,j_\mathsf{D})\in\mathcal{S}_1} \Theta_{i,j_\mathsf{D}}^{(\kappa)}(\mathbf{V}_\mathsf{D}, \mathbf{V}_\mathsf{U}, \boldsymbol{\alpha}_{i,j_\mathsf{D}}) \tag{23a}$$

$$\text{s.t. (13b)} - \text{(13e)} \tag{23b}$$

$$\phi_{i,j_\mathsf{D}}^{(\kappa)}(\mathbf{V}_\mathsf{D}, \mathbf{V}_\mathsf{U}) \geq e_{i,j_\mathsf{D}}^{\min}/\zeta_{i,j_\mathsf{D}}(1-\boldsymbol{\alpha}_{i,j_\mathsf{D}}), \quad \forall (i, j_\mathsf{D}) \in \mathcal{S}_1, \tag{23c}$$

$$\Theta_i^{(\kappa)}(\mathbf{V}_\mathsf{D}, \mathbf{V}_\mathsf{U}) \geq r_i^{\mathsf{U},\min}, \quad \forall i \in I, \tag{23d}$$

$$\Theta_{i,j_\mathsf{D}}^{(\kappa)}(\mathbf{V}_\mathsf{D}, \mathbf{V}_\mathsf{U}, \boldsymbol{\alpha}_{i,j_\mathsf{D}}) \geq r_{i,j_\mathsf{D}}^{\mathsf{D},\min}, \quad \forall (i, j_\mathsf{D}) \in \mathcal{S}_1. \tag{23e}$$

Initializing from $(V_\mathsf{D}^{(\kappa)}, V_\mathsf{U}^{(\kappa)}, \alpha^{(\kappa)})$ being a feasible point for (13), the optimal solution $(V_\mathsf{D}^{(\kappa+1)}, V_\mathsf{U}^{(\kappa+1)}, \alpha^{(\kappa+1)})$ of the convex program (23) is feasible for the nonconvex program (13) and it is better than $(V_\mathsf{D}^{(\kappa)}, V_\mathsf{U}^{(\kappa)}, \alpha^{(\kappa)})$:

$$\begin{aligned} \mathcal{P}_1(V_\mathsf{D}^{(\kappa+1)}, V_\mathsf{U}^{(\kappa+1)}, \alpha^{(\kappa+1)}) &\geq \\ \mathcal{P}_1^{(\kappa)}(V_\mathsf{D}^{(\kappa+1)}, V_\mathsf{U}^{(\kappa+1)}, \alpha^{(\kappa+1)}) &\geq \quad (24) \\ \mathcal{P}_1^{(\kappa)}(V_\mathsf{D}^{(\kappa)}, V_\mathsf{U}^{(\kappa)}, \alpha^{(\kappa)}) &= \quad (25) \\ \mathcal{P}_1(V_\mathsf{D}^{(\kappa)}, V_\mathsf{U}^{(\kappa)}, \alpha^{(\kappa)}), & \quad (26) \end{aligned}$$

where the inequality (24) and the equality (26) follow from the fact that $\mathcal{P}_1^{(\kappa)}$ is a minorant of $\mathcal{P}_1$ while the inequality (25) follows from the fact that $(V_\mathsf{D}^{(\kappa+1)}, V_\mathsf{U}^{(\kappa+1)}, \alpha^{(\kappa+1)})$ and $(V_\mathsf{D}^{(\kappa)}, V_\mathsf{U}^{(\kappa)}, \alpha^{(\kappa)})$ are the optimal solution and a feasible point of (23), respectively. This generates a sequence $\{(V_\mathsf{D}^{(\kappa)}, V_\mathsf{U}^{(\kappa)}, \alpha^{(\kappa)})\}$ of feasible and improved points which converges to a local optimum of (13) after finitely many iterations [16].

Algorithm 1 Path-Following Algorithm for PS Sum Throughput Maximization (13)

Initialization: Set $\kappa := 0$, and choose a feasible point $(V_\mathsf{D}^{(0)}, V_\mathsf{U}^{(0)}, \alpha^{(0)})$ that satisfies (13b)-(13h).

κ-th iteration: Solve (23) for an optimal solution $(V_\mathsf{D}^*, V_\mathsf{U}^*, \alpha^*)$ and set $\kappa := \kappa + 1$, $(V_\mathsf{D}^{(\kappa)}, V_\mathsf{U}^{(\kappa)}, \alpha^{(\kappa)}) := (V_\mathsf{D}^*, V_\mathsf{U}^*, \alpha^*)$ and calculate $\mathcal{P}_1(V_\mathsf{D}^{(\kappa)}, V_\mathsf{U}^{(\kappa)}, \alpha^{(\kappa)})$. Stop if $\left|\left(\mathcal{P}_1(V_\mathsf{D}^{(\kappa)}, V_\mathsf{U}^{(\kappa)}, \alpha^{(\kappa)}) - \mathcal{P}_1(V_\mathsf{D}^{(\kappa-1)}, V_\mathsf{U}^{(\kappa-1)}, \alpha^{(\kappa-1)})\right) / \mathcal{P}_1(V_\mathsf{D}^{(\kappa-1)}, V_\mathsf{U}^{(\kappa-1)}, \alpha^{(\kappa-1)})\right| \leq \epsilon$.

The proposed path-following procedure that solves problem (13) is summarized in Algorithm 1. To find a feasible initial point $(V_\mathsf{D}^{(0)}, V_\mathsf{U}^{(0)}, \alpha^{(0)})$ meeting the nonconvex constraints (13f)-(13h) we consider the following problem:

$$\begin{aligned} &\max_{\mathbf{V}_\mathsf{D}, \mathbf{V}_\mathsf{U}, \boldsymbol{\alpha}} \ \mathcal{P}_{1,f}(\mathbf{V}_\mathsf{D}, \mathbf{V}_\mathsf{U}, \boldsymbol{\alpha}) \triangleq \\ &\min_{(i,j_\mathsf{D})\in\mathcal{S}_1} \left\{\Phi_{i,j_\mathsf{D}}(\mathbf{V}_\mathsf{D}, \mathbf{V}_\mathsf{U}) - \frac{e_{i,j_\mathsf{D}}^{\min}}{\zeta_{i,j_\mathsf{D}}(1-\boldsymbol{\alpha}_{i,j_\mathsf{D}})}, \right. \\ &\qquad \left. f_{i,j_\mathsf{D}}(\mathbf{V}_\mathsf{D}, \mathbf{V}_\mathsf{U}, \boldsymbol{\alpha}) - r_{i,i_\mathsf{D}}^{\min}, f_i(\mathbf{V}_\mathsf{D}, \mathbf{V}_\mathsf{U}) - r_i^{\min}\right\} \\ &\text{s.t. (13b)} - \text{(13e)}. \end{aligned} \tag{27}$$

Initialized by a $(V_\mathsf{D}^{(0)}, V_\mathsf{U}^{(0)}, \alpha^{(0)})$ feasible for the convex constraints (13b)-(13e), an iterative point $(V_\mathsf{D}^{(\kappa+1)}, V_\mathsf{U}^{(\kappa+1)}, \alpha^{(\kappa+1)})$ for $\kappa = 0, 1, \ldots$, is generated as the optimal solution of the following convex maximin program:

$$\begin{aligned} &\max_{\mathbf{V}_\mathsf{D}, \mathbf{V}_\mathsf{U}, \boldsymbol{\alpha}} \ \mathcal{P}_{1,f}^{(\kappa)}(\mathbf{V}_\mathsf{D}, \mathbf{V}_\mathsf{U}, \boldsymbol{\alpha}) \triangleq \\ &\min_{(i,j_\mathsf{D})\in\mathcal{S}_1} \left\{\phi_{i,j_\mathsf{D}}^{(\kappa)}(\mathbf{V}_\mathsf{D}, \mathbf{V}_\mathsf{U}) - \frac{e_{i,j_\mathsf{D}}^{\min}}{\zeta_{i,j_\mathsf{D}}(1-\boldsymbol{\alpha}_{i,j_\mathsf{D}})}, \right. \\ &\qquad \left. \langle \Theta_{i,j_\mathsf{D}}^{(\kappa)}(\mathbf{V}_\mathsf{D}, \mathbf{V}_\mathsf{U}, \boldsymbol{\alpha}) - r_{i,i_\mathsf{D}}^{\min}, \Theta_i^{(\kappa)}(\mathbf{V}_\mathsf{D}, \mathbf{V}_\mathsf{U}) - r_i^{\min}, \right\} \\ &\text{s.t} \quad \text{(13b)} - \text{(13e)}. \end{aligned} \tag{28}$$

which terminates upon reaching

$$f_{i,j_\mathsf{D}}(V_\mathsf{D}^{(\kappa)}, V_\mathsf{U}^{(\kappa)}, \alpha^{(\kappa)}) \geq r_{i,i_\mathsf{D}}^{\min}, \quad f_i(V_\mathsf{D}^{(\kappa)}, V_\mathsf{U}^{(\kappa)}) \geq r_i^{\min}, \quad \langle \Phi_{i,j_\mathsf{D}}(V_\mathsf{D}^{(\kappa)}, V_\mathsf{U}^{(\kappa)})\rangle \geq \frac{e_{i,j_\mathsf{D}}^{\min}}{\zeta_{i,j_\mathsf{D}}(1-\boldsymbol{\alpha}_{i,j_\mathsf{D}})}, \quad \forall (i, j_\mathsf{D}) \in \mathcal{S}_1$$

to satisfy (13b)-(13h).

In parallel, we consider the following transmission strategy to configure FD BSs to operate in the HD mode. Here, all $N = N_1 + N_2$ antennas at each BS are used to serve all the DLUs in the downlink and all the ULUs in the uplink using half time slots, where DLUs are allowed to harvest energy from ULUs. The problem can be formulated as

$$\max_{\mathbf{V}_\mathsf{D},\mathbf{V}_\mathsf{U},\boldsymbol{\alpha}} \frac{1}{2}\Big[\sum_{(i,j_\mathsf{D})\in\mathcal{S}_1} f_{i,j_\mathsf{D}}(\mathbf{V}_\mathsf{D},0_\mathsf{U},\boldsymbol{\alpha}_{i,j_\mathsf{D}}) + \sum_{i\in I} f_i(0_\mathsf{D},\mathbf{V}_\mathsf{U})\Big] \tag{29a}$$

s.t. (13b), (13c), (13d), (13e),

$$\frac{1}{2}(E_{i,j_\mathsf{D}}(\mathbf{V}_\mathsf{D},0_\mathsf{U},\boldsymbol{\alpha}_{i,j_\mathsf{D}}) + E_{i,j_\mathsf{D}}(0_\mathsf{D},\mathbf{V}_\mathsf{U},0)) \geq e^{\min}_{i,j_\mathsf{D}}, \quad \forall (i,j_\mathsf{D})\in\mathcal{S}_1, \tag{29b}$$

$$\frac{1}{2} f_i(0_\mathsf{D},\mathbf{V}_\mathsf{U}) \geq r_i^{\mathsf{U},\min}, \quad \forall i\in I \tag{29c}$$

$$\frac{1}{2} f_{i,j_\mathsf{D}}(\mathbf{V}_\mathsf{D},0_\mathsf{U},\boldsymbol{\alpha}_{i,j_\mathsf{D}}) \geq r_{i,j_\mathsf{D}}^{\mathsf{D},\min}, \quad \forall (i,j_\mathsf{D})\in\mathcal{S}_1, \tag{29d}$$

where 0_D and 0_U are all-zero quantities of the same dimension as $\mathbf{V}_\mathsf{D}$ and $\mathbf{V}_\mathsf{U}$. In (29), DLU (i, j_D) uses $(1-\boldsymbol{\alpha}_{i,j_\mathsf{D}})$ of the received signal during DL transmission and the whole received signal during UL transmission for EH as formulated in (29b). The main difference between (13) and (29) is in (29b) where the harvested energy from UL transmission at DLU (i, j_D) is not multiplied by $\boldsymbol{\alpha}_{i,j_\mathsf{D}}$. The constraint (29b) can be recast as

$$\langle \Phi_{i,j_\mathsf{D}}(\mathbf{V}_\mathsf{D},0_\mathsf{U})\rangle + \frac{\langle \Phi_{i,j_\mathsf{D}}(0_\mathsf{D},\mathbf{V}_\mathsf{U})\rangle}{(1-\boldsymbol{\alpha}_{i,j_\mathsf{D}})} \geq \frac{2e^{\min}_{i,j_\mathsf{D}}}{\zeta_{i,j_\mathsf{D}}(1-\boldsymbol{\alpha}_{i,j_\mathsf{D}})}.$$

Define the following convex function:

$$\Lambda_{i,j_\mathsf{D}}(\mathbf{V}_\mathsf{U},\boldsymbol{\alpha}_{i,j_\mathsf{D}}) \triangleq \frac{\langle \Phi_{i,j_\mathsf{D}}(0_\mathsf{D},\mathbf{V}_\mathsf{U})\rangle}{(1-\boldsymbol{\alpha}_{i,j_\mathsf{D}})} = \frac{\langle \sum_{\ell_\mathsf{U}\in\mathcal{U}}(H_{i,j_\mathsf{D},\ell_\mathsf{U}}\mathbf{V}_{i,\ell_\mathsf{U}})^2 + \sigma_\mathsf{D}^2 I_{N_r}\rangle}{1-\boldsymbol{\alpha}_{i,j_\mathsf{D}}}, \tag{30}$$

with its first-order approximation

$$\Lambda^{(\kappa)}_{i,j_\mathsf{D}}(\mathbf{V}_\mathsf{U},1-\boldsymbol{\alpha}_{i,j_\mathsf{D}}) \triangleq \frac{2\Re\{\langle \sum_{\ell_\mathsf{U}\in\mathcal{U}}(H_{i,j_\mathsf{D},\ell_\mathsf{U}}\mathbf{V}_{i,\ell_\mathsf{U}})(H_{i,j_\mathsf{D},\ell_\mathsf{U}}V^{(\kappa)}_{i,\ell_\mathsf{U}})^H\rangle\}}{1-\alpha^{(\kappa)}_{i,j_\mathsf{D}}} - \frac{\langle \sum_{\ell_\mathsf{U}\in\mathcal{U}}(H_{i,j_\mathsf{D},\ell_\mathsf{U}}V^{(\kappa)}_{i,\ell_\mathsf{U}})^2 + \sigma_\mathsf{D}^2 I_{N_r}\rangle}{(1-\alpha^{(\kappa)}_{i,j_\mathsf{D}})^2}(1-\boldsymbol{\alpha}_{i,j_\mathsf{D}}), \tag{31}$$

which is its minorant at $(V^{(\kappa)}_\mathsf{D}, V^{(\kappa)}_\mathsf{U}, \alpha^{(\kappa)})$.

Algorithm 1 can be used with the following convex program solved at the κ^{th} iteration:

$$\max_{\mathbf{V}_\mathsf{D},\mathbf{V}_\mathsf{U},\boldsymbol{\alpha}} \frac{1}{2}\Big[\sum_{(i,j_\mathsf{D})\in\mathcal{S}_1} \Theta^{(\kappa)}_{i,j_\mathsf{D}}(\mathbf{V}_\mathsf{D},0_\mathsf{U},\boldsymbol{\alpha}_{i,j_\mathsf{D}}) + \sum_{i\in I}\Theta^{(\kappa)}_i(0_\mathsf{D},\mathbf{V}_\mathsf{U},0)\Big] \tag{32a}$$

s.t. (13b), (13c), (13d), (13e),

$$\phi^{(\kappa)}_{i,j_\mathsf{D}}(\mathbf{V}_\mathsf{D},0_\mathsf{U}) + \Lambda^{(\kappa)}_{i,j_\mathsf{D}}(\mathbf{V}_\mathsf{U},1-\boldsymbol{\alpha}_{i,j_\mathsf{D}}) \geq \frac{2e^{\min}_{i,j_\mathsf{D}}}{\zeta_{i,j_\mathsf{D}}(1-\boldsymbol{\alpha}_{i,j_\mathsf{D}})}, \forall (i,j_\mathsf{D})\in\mathcal{S}_1, \tag{32b}$$

$$\frac{1}{2}\Theta^{(\kappa)}_i(0_\mathsf{D},\mathbf{V}_\mathsf{U}) \geq r_i^{\mathsf{U},\min}, \forall i\in I \tag{32c}$$

$$\frac{1}{2}\Theta^{(\kappa)}_{i,j_\mathsf{D}}(\mathbf{V}_\mathsf{D},0_\mathsf{U},\boldsymbol{\alpha}_{i,j_\mathsf{D}}) \geq r_{i,j_\mathsf{D}}^{\mathsf{D},\min}, \quad \forall (i,j_\mathsf{D})\in\mathcal{S}_1, \tag{32d}$$

where $\phi^{(\kappa)}_{i,j_\mathsf{D}}(\mathbf{V}_\mathsf{D},0_\mathsf{U})$ and $\Theta^{(\kappa)}_{i,j_\mathsf{D}}(\mathbf{V}_\mathsf{D},0_\mathsf{U},\boldsymbol{\alpha}_{i,j_\mathsf{D}})$ are defined by (22) and (18) with both $\mathbf{V}_\mathsf{U}$ and $V^{(\kappa)}_\mathsf{U}$ replaced by 0_U, while $\Theta^{(\kappa)}_i(0_\mathsf{D},\mathbf{V}_\mathsf{U})$ is defined by (19) with both $\mathbf{V}_\mathsf{D}$ and $V^{(\kappa)}_\mathsf{D}$ replaced by 0_D.

Problems (23), (28) and (32) involve $n = 2(N_1 d_1 ID + N_r d_2 IU) + ID$ scalar real decision variables and $m = 5ID + IU + 2I + 1$ quadratic constraints so their computational complexity is $O(n^2 m^{2.5} + m^{3.5})$.

III. EH-Enabled FD MU-MIMO by TS

A much easier implementation is time splitting in the downlink transmission where $(1-\boldsymbol{\alpha})$ of the time is used for DL energy transfer and $\boldsymbol{\alpha}$ of the time is used for DL information transmission, with $0 < \boldsymbol{\alpha} < 1$. In this section, we define $\mathbf{V}^I_\mathsf{D} \triangleq [\mathbf{V}^I_{i,j_\mathsf{D}}]_{(i,j_\mathsf{D})\in\mathcal{S}_1}$, $\mathbf{V}^E_\mathsf{D} \triangleq [\mathbf{V}^E_{i,j_\mathsf{D}}]_{(i,j_\mathsf{D})\in\mathcal{S}_1}$ and redefine the notation $\mathbf{V}_\mathsf{D} \triangleq [\mathbf{V}^I_\mathsf{D}, \mathbf{V}^E_\mathsf{D}]$ where $\mathbf{V}^I_{i,j_\mathsf{D}}$ and $\mathbf{V}^E_{i,j_\mathsf{D}}$ are the information precoding matrix for ID and energy precoding matrix for EH, respectively. The received signal at DLU (i, j_D) for EH is

$$y^E_{i,j_\mathsf{D}} \triangleq \sum_{(m,\ell_\mathsf{D})\in\mathcal{S}_1} H_{m,i,j_\mathsf{D}}\mathbf{V}^E_{m,\ell_\mathsf{D}}s^E_{m,\ell_\mathsf{D}} + \underbrace{\sum_{\ell_\mathsf{U}\in\mathcal{U}} H_{i,j_\mathsf{D},\ell_\mathsf{U}}\mathbf{V}_{i,\ell_\mathsf{U}}s_{i,\ell_\mathsf{U}}}_{\text{UL intracell interference}} + n_{j_\mathsf{D}}, \tag{33}$$

where s^E_{m,ℓ_D} is the energy signal sent during $(1-\boldsymbol{\alpha})$ of the time. With the definition (6), the harvested energy is

$$E_{i,j_\mathsf{D}}(\mathbf{V}^E_\mathsf{D},\mathbf{V}_\mathsf{U},\boldsymbol{\alpha}) = \zeta_{i,j_\mathsf{D}}(1-\boldsymbol{\alpha})\langle \Phi_{i,j_\mathsf{D}}(\mathbf{V}^E_\mathsf{D},\mathbf{V}_\mathsf{U})\rangle,$$

where the downlink signal covariance mapping $\Phi_{i,j_\mathsf{D}}(\cdot,\cdot)$ is defined from (7).

Similarly to (1), the signal received at DLU (i, j_D) during the information transmission in time fraction $\boldsymbol{\alpha}$ is

$$y^I_{i,j_\mathsf{D}} \triangleq \underbrace{H_{i,i,j_\mathsf{D}}\mathbf{V}_{i,j_\mathsf{D}}s^I_{i,j_\mathsf{D}}}_{\text{desired signal}} + \underbrace{\sum_{(m,\ell_\mathsf{D})\in\mathcal{S}_1\setminus(i,j_\mathsf{D})} H_{m,i,j_\mathsf{D}}\mathbf{V}_{m,\ell_\mathsf{D}}s^I_{m,\ell_\mathsf{D}}}_{\text{DL interference}} + \underbrace{\sum_{\ell_\mathsf{U}\in\mathcal{U}} H_{i,j_\mathsf{D},\ell_\mathsf{U}}\mathbf{V}_{i,\ell_\mathsf{U}}s_{i,\ell_\mathsf{U}}}_{\text{UL intracell interference}} + n_{i,j_\mathsf{D}}, \tag{34}$$

where s^I_{m,ℓ_D} is the information signal intended for DLU (m, ℓ_D). The ID throughput at DLU (i, j_D) is then given

as $\boldsymbol{\alpha} f_{i,j_\mathsf{D}}(\mathbf{V})$, where

$$f_{i,j_\mathsf{D}}(\mathbf{V}_\mathsf{D}^I, \mathbf{V}_\mathsf{U}) = \ln\left|I_{N_r} + (\mathcal{L}_{i,j_\mathsf{D}}(\mathbf{V}_{i,j_\mathsf{D}}^I))^2 \bar{\Psi}_{i,j_\mathsf{D}}^{-1}(\mathbf{V}_\mathsf{D}^I, \mathbf{V}_\mathsf{U})\right|, \tag{35}$$

with the downlink interference covariance mapping $\bar{\Psi}(\cdot,\cdot)$ defined from (5).

The uplink throughput at the BS is

$$f_i(\mathbf{V}_\mathsf{D}, \mathbf{V}_\mathsf{U}, \boldsymbol{\alpha}) \triangleq \ln\left|I_{N_2} + (\mathcal{L}_i(\mathbf{V}_{\mathsf{U}_i}))^2 s \Psi_i^{-1}(\mathbf{V}_\mathsf{D}, \mathbf{V}_\mathsf{U}, \boldsymbol{\alpha})\right|, \tag{36}$$

where $\mathcal{L}_i(\mathbf{V}_{\mathsf{U}_i})$ is already defined from (9) but

$$\Psi_i(\mathbf{V}_\mathsf{D}, \mathbf{V}_\mathsf{U}, \boldsymbol{\alpha}) \triangleq \bar{\Psi}_i^U(\mathbf{V}_\mathsf{U}) + \bar{\Psi}_i^{TSI}(\mathbf{V}_\mathsf{D}, \boldsymbol{\alpha}) \tag{37}$$

with the uplink interference covariance mapping $\bar{\Psi}_i^U(\cdot)$ defined by (11) and the time-splitting SI covariance mapping

$$\bar{\Psi}_i^{TSI}(\mathbf{V}_\mathsf{D}, \boldsymbol{\alpha}) \triangleq \sigma_{SI}^2 \sum_{j_\mathsf{D}\in\mathcal{D}} \left((1-\boldsymbol{\alpha})||\mathbf{V}_{i,j_\mathsf{D}}^E||^2 + \boldsymbol{\alpha}||\mathbf{V}_{i,j_\mathsf{D}}^I||^2\right) I_{N_2}. \tag{38}$$

The problem of maximizing the network total throughput under throughput QoS and EH constraints is the following:

$$\max_{\mathbf{V}_\mathsf{D},\mathbf{V}_\mathsf{U},\boldsymbol{\alpha}} \ \mathcal{P}_2(\mathbf{V}_\mathsf{D}, \mathbf{V}_\mathsf{U}, \boldsymbol{\alpha}) \triangleq$$

$$\sum_{(i,j_\mathsf{D})\in\mathcal{S}_1} \left(\boldsymbol{\alpha} f_{i,j_\mathsf{D}}(\mathbf{V}_\mathsf{D}^I, \mathbf{V}_\mathsf{U}) + f_i(\mathbf{V}_\mathsf{D}, \mathbf{V}_\mathsf{U}, \boldsymbol{\alpha})\right) \tag{39a}$$

$$\text{s.t. } 0 < \boldsymbol{\alpha} < 1, \tag{39b}$$

$$||\mathbf{V}_{i,j_\mathsf{U}}||^2 \le P_{i,j_\mathsf{U}}, \quad \forall (i,j_\mathsf{U}) \in \mathcal{S}_2, \tag{39c}$$

$$\sum_{(i,j_\mathsf{D})\in\mathcal{S}_1} \left((1-\boldsymbol{\alpha})||\mathbf{V}_{i,j_\mathsf{D}}^E||^2 + \boldsymbol{\alpha}||\mathbf{V}_{i,j_\mathsf{D}}^I||^2\right) + \sum_{(i,j_\mathsf{U})\in\mathcal{S}_2} ||\mathbf{V}_{i,j_\mathsf{U}}||^2 \le P, \tag{39d}$$

$$\sum_{j_\mathsf{D}\in\mathcal{D}} \left((1-\boldsymbol{\alpha})||\mathbf{V}_{i,j_\mathsf{D}}^E||^2 + \boldsymbol{\alpha}||\mathbf{V}_{i,j_\mathsf{D}}^I||^2\right) \le P_i, \quad \forall i \in I, \tag{39e}$$

$$f_i(\mathbf{V}_\mathsf{D}, \mathbf{V}_\mathsf{U}, \boldsymbol{\alpha}) \ge r_i^{\mathsf{U},\min}, \quad \forall i \in I, \tag{39f}$$

$$\boldsymbol{\alpha} f_{i,j_\mathsf{D}}(\mathbf{V}_\mathsf{D}^I, \mathbf{V}_\mathsf{U}) \ge r_{i,j_\mathsf{D}}^{\mathsf{D},\min}, \quad \forall (i,j_\mathsf{D}) \in \mathcal{S}_1, \tag{39g}$$

$$E_{i,j_\mathsf{D}}(\mathbf{V}_\mathsf{D}^E, \mathbf{V}_\mathsf{U}, \boldsymbol{\alpha}) \ge e_{i,j_\mathsf{D}}^{\min}, \quad \forall (i,j_\mathsf{D}) \in \mathcal{S}_1. \tag{39h}$$

Constraints (39c), (39d) and (39e) limits the transmit power of each ULU, the whole network and each BS, respectively. Constraints (39h) ensure that each DLU harvests more than a threshold, whereas constraints (39f) and (39g) guarantee the throughput QoS at the BSs and DLUs, respectively. The key difficulty in problem (39) is to handle the time splitting factor $\boldsymbol{\alpha}$ that is coupled with the objective functions and other variables. Using the variable change $\boldsymbol{\rho} = 1/\boldsymbol{\alpha}$, which satisfies the convex constraint

$$\boldsymbol{\rho} > 1, \tag{40}$$

problem (39) is equivalent to

$$\max_{\mathbf{V}_\mathsf{D},\mathbf{V}_\mathsf{U},\boldsymbol{\rho}>0} \mathcal{P}_2(\mathbf{V}_\mathsf{D}, \mathbf{V}_\mathsf{U}, \boldsymbol{\rho}) \triangleq$$

$$\sum_{(i,j_\mathsf{D})\in\mathcal{S}_1} f_{i,j_\mathsf{D}}(\mathbf{V}_\mathsf{D}^I, \mathbf{V}_\mathsf{U})/\boldsymbol{\rho} + \sum_{i\in I} f_i(\mathbf{V}_\mathsf{D}, \mathbf{V}_\mathsf{U}, 1/\boldsymbol{\rho}) \tag{41a}$$

$$\text{s.t. (40), (39c),}$$

$$\sum_{(i,j_\mathsf{D})\in\mathcal{S}_1} \left(||\mathbf{V}_{i,j_\mathsf{D}}^E||^2 + ||\mathbf{V}_{i,j_\mathsf{D}}^I||^2/\boldsymbol{\rho}\right) + \sum_{(i,j_\mathsf{U})\in\mathcal{S}_2} ||\mathbf{V}_{i,j_\mathsf{U}}||^2 \le P + \sum_{(i,j_\mathsf{D})\in\mathcal{S}_1} ||\mathbf{V}_{i,j_\mathsf{D}}^E||^2/\boldsymbol{\rho}, \tag{41b}$$

$$\sum_{j_\mathsf{D}\in\mathcal{D}} \left(||\mathbf{V}_{i,j_\mathsf{D}}^E||^2 + ||\mathbf{V}_{i,j_\mathsf{D}}^I||^2/\boldsymbol{\rho}\right) \le P_i + \sum_{j_\mathsf{D}\in\mathcal{D}} ||\mathbf{V}_{i,j_\mathsf{D}}^E||^2/\boldsymbol{\rho}, \quad \forall i \in I, \tag{41c}$$

$$E_{i,j_\mathsf{D}}(\mathbf{V}_\mathsf{D}^E, \mathbf{V}_\mathsf{U}, 1/\boldsymbol{\rho}) \ge e_{i,j_\mathsf{D}}^{\min}, \quad \forall (i,j_\mathsf{D}) \in \mathcal{S}_1, \tag{41d}$$

$$f_i(\mathbf{V}_\mathsf{D}, \mathbf{V}_\mathsf{U}, 1/\boldsymbol{\rho}) \ge r_i^{\mathsf{U},\min}, \quad \forall i \in I, \tag{41e}$$

$$f_{i,j_\mathsf{D}}(\mathbf{V}_\mathsf{D}^I, \mathbf{V}_\mathsf{U})/\boldsymbol{\rho} \ge r_{i,j_\mathsf{D}}^{\mathsf{D},\min}, \quad \forall (i,j_\mathsf{D}) \in \mathcal{S}_1. \tag{41f}$$

Problem (41) is much more difficult computationally than (13). Firstly, the DL throughput is now the multiplication of data throughput and the portion of time $1/\boldsymbol{\rho}$. Secondly, the SI in UL throughput is also coupled with $1/\boldsymbol{\rho}$. Finally, the power constraints (41b) and (41c) are also coupled with $1/\boldsymbol{\rho}$. Therefore, the objective function (41a) and constraints (41b)-(41f) are all nonconvex and cannot be addressed as in (13). In the following, we will develop the new minorants of the DL throughput function and UL throughput function.

Firstly, we address a lower approximation for each $f_{i,j_\mathsf{D}}(\mathbf{V}_\mathsf{D}^I, \mathbf{V}_\mathsf{U})/\boldsymbol{\rho}$ in (41a) and (41f). Recalling the definition (35) of $f_{i,j_\mathsf{D}}(\mathbf{V}_\mathsf{D}^I, \mathbf{V}_\mathsf{U})$ we introduce

$$\mathcal{M}_{i,j_\mathsf{D}}(\mathbf{V}_\mathsf{D}^I, \mathbf{V}_\mathsf{U}) \triangleq (\mathcal{L}_{i,j_\mathsf{D}}(\mathbf{V}_{i,j_\mathsf{D}}))^2 + \bar{\Psi}_{i,j_\mathsf{D}}(\mathbf{V}_\mathsf{D}, \mathbf{V}_\mathsf{U}),$$

to have its following minorant at $(V_\mathsf{D}^{(\kappa)}, V_\mathsf{U}^{(\kappa)})$:

$$\Theta_{i,j_\mathsf{D}}^{(\kappa)}(\mathbf{V}_\mathsf{D}^I, \mathbf{V}_\mathsf{U}) \triangleq a_{i,j_\mathsf{D}}^{(\kappa)} + 2\Re\left\{\langle \mathcal{A}_{i,j_\mathsf{D}}^{(\kappa)}, \mathcal{L}_{i,j_\mathsf{D}}(\mathbf{V}_{i,j_\mathsf{D}}^I)\rangle\right\} - \langle \mathcal{B}_{i,j_\mathsf{D}}^{(\kappa)}, \mathcal{M}_{i,j_\mathsf{D}}(\mathbf{V}_\mathsf{D}^I, \mathbf{V}_\mathsf{U})\rangle, \tag{42}$$

where similarly to (20)

$$\begin{aligned} 0 > a_{i,j_\mathsf{D}}^{(\kappa)} &= f_{i,j_\mathsf{D}}(V_\mathsf{D}^{(\kappa)}, V_\mathsf{U}^{(\kappa)}) \\ &\quad - \Re\left\{\langle \bar{\Psi}_{i,j_\mathsf{D}}^{-1}(V_\mathsf{D}^{(\kappa)}, V_\mathsf{U}^{(\kappa)}) \mathcal{L}_{i,j_\mathsf{D}}(V_{i,j_\mathsf{D}}^{(\kappa)}), \right. \\ &\qquad \left. \mathcal{L}_{i,j_\mathsf{D}}(V_{i,j_\mathsf{D}}^{(\kappa)})\rangle\right\}, \\ \mathcal{A}_{i,j_\mathsf{D}}^{(\kappa)} &= \bar{\Psi}_{i,j_\mathsf{D}}^{-1}(V_\mathsf{D}^{(\kappa)}, V_\mathsf{U}^{(\kappa)}) \mathcal{L}_{i,j_\mathsf{D}}(V_{i,j_\mathsf{D}}^{(\kappa)}), \\ 0 \preceq \mathcal{B}_{i,j_\mathsf{D}}^{(\kappa)} &= \bar{\Psi}_{i,j_\mathsf{D}}^{-1}(V_\mathsf{D}^{(\kappa)}, V_\mathsf{U}^{(\kappa)}) - \mathcal{M}_{i,j_\mathsf{D}}^{-1}(V_\mathsf{D}^{(\kappa)}, V_\mathsf{U}^{(\kappa)}). \end{aligned} \tag{43}$$

A minorant of $f_{i,j_\mathsf{D}}(\mathbf{V}_\mathsf{D}^I, \mathbf{V}_\mathsf{U})/\boldsymbol{\rho}$ is $\Theta_{i,j_\mathsf{D}}^{(\kappa)}(\mathbf{V}_\mathsf{D}^I, \mathbf{V}_\mathsf{U})/\boldsymbol{\rho}$ but it is still not concave. As $f_{i,j_\mathsf{D}}(\mathbf{V}_\mathsf{D}^I, \mathbf{V}_\mathsf{U}) > 0$ it is obvious that its lower bound $\Theta_{i,j_\mathsf{D}}^{(\kappa)}(\mathbf{V}_\mathsf{D}^I, \mathbf{V}_\mathsf{U})$ is meaningful for $(\mathbf{V}_\mathsf{D}^I, \mathbf{V}_\mathsf{U})$ such that

$$\Theta_{i,j_\mathsf{D}}^{(\kappa)}(\mathbf{V}_\mathsf{D}^I, \mathbf{V}_\mathsf{U}) \ge 0, \ (i,j_\mathsf{D}) \in \mathcal{S}_1 \tag{44}$$

which particularly implies

$$\Re\left\{\left\langle(\mathcal{A}_{i,j_\mathsf{D}}^{(\kappa)}, \mathcal{L}_{i,j_\mathsf{D}}(\mathbf{V}_{i,j_\mathsf{D}}^{I})\right\rangle\right\} \geq 0,\ \ (i, j_\mathsf{D}) \in \mathcal{S}_1. \tag{45}$$

Under (45), we have

$$\frac{\Re\left\{\langle\mathcal{A}_{i,j_\mathsf{D}}^{(\kappa)}, \mathcal{L}_{i,j_\mathsf{D}}(\mathbf{V}_{i,j_\mathsf{D}}^{I})\rangle\right\}}{\boldsymbol{\rho}} \geq 2b_{i,j_\mathsf{D}}^{(\kappa)}\sqrt{\Re\left\{\langle\mathcal{A}_{i,j_\mathsf{D}}^{(\kappa)}, \mathcal{L}_{i,j_\mathsf{D}}(\mathbf{V}_{i,j_\mathsf{D}}^{I})\rangle\right\}} - c_{i,j_\mathsf{D}}^{(\kappa)}\boldsymbol{\rho} \tag{46}$$

for

$$0 < b_{i,j_\mathsf{D}}^{(\kappa)} = \frac{\sqrt{\langle\mathcal{A}_{i,j_\mathsf{D}}^{(\kappa)}, \mathcal{L}_{i,j_\mathsf{D}}(V_{i,j_\mathsf{D}}^{I,(\kappa)})\rangle}}{\rho^{(\kappa)}},$$
$$0 < c_{i,j_\mathsf{D}}^{(\kappa)} = (b_{i,j_\mathsf{D}}^{(\kappa)})^2. \tag{47}$$

Therefore, the following concave function:

$$g_{i,j_\mathsf{D}}^{(\kappa)}(\mathbf{V}_\mathsf{D}^{I}, \mathbf{V}_\mathsf{U}, \boldsymbol{\rho}) \quad \frac{a_{i,j_\mathsf{D}}^{(\kappa)}}{\boldsymbol{\rho}} + \triangleq 4b_{i,j_\mathsf{D}}^{(\kappa)}\sqrt{\Re\left\{\langle\mathcal{A}_{i,j_\mathsf{D}}^{(\kappa)}, \mathcal{L}_{i,j_\mathsf{D}}(\mathbf{V}_{i,j_\mathsf{D}}^{I})\rangle\right\}} - 2c_{i,j_\mathsf{D}}^{(\kappa)}\boldsymbol{\rho} - \frac{\langle\mathcal{B}^{(\kappa)}, \mathcal{M}_{i,j_\mathsf{D}}(\mathbf{V}_\mathsf{D}^{I}, \mathbf{V}_\mathsf{U})\rangle}{\boldsymbol{\rho}} \tag{48}$$

is a minorant of $f_{i,j_\mathsf{D}}(\mathbf{V}_\mathsf{D}^{I}, \mathbf{V}_\mathsf{U})/\boldsymbol{\rho}$ at $(V_\mathsf{D}^{I,(\kappa)}, V_\mathsf{U}^{(\kappa)}, \rho^{(\kappa)})$.

Next, we address a lower approximation of $f_i(\mathbf{V}_\mathsf{D}, \mathbf{V}_\mathsf{U}, 1/\boldsymbol{\rho})$ in (41a) and (41e). Recalling the definition (36) of $f_i(\mathbf{V}_\mathsf{D}, \mathbf{V}_\mathsf{U}, 1/\boldsymbol{\rho})$ we introduce

$$\mathcal{M}_i(\mathbf{V}_\mathsf{D}, \mathbf{V}_\mathsf{U}, \boldsymbol{\rho}) \triangleq (\mathcal{L}_i(\mathbf{V}_{\mathsf{U}i}))^2 + \bar{\Psi}_i^{U}(\mathbf{V}_\mathsf{U}) + \bar{\Psi}_i^{TSI}(\mathbf{V}_\mathsf{D}, 1/\boldsymbol{\rho}), \tag{49}$$

for $\bar{\Psi}_i^{TSI}(\mathbf{V}_\mathsf{D}, 1/\boldsymbol{\rho})$ defined from (38) as

$$\bar{\Psi}_i^{TSI}(\mathbf{V}_\mathsf{D}, 1/\boldsymbol{\rho}) = \sigma_{SI}^2\sum_{j_\mathsf{D}\in\mathcal{D}}\Big(||\mathbf{V}_{i,j_\mathsf{D}}^{E}||^2 + \frac{1}{\boldsymbol{\rho}}||\mathbf{V}_{i,j_\mathsf{D}}^{I}||^2 - \frac{1}{\boldsymbol{\rho}}||\mathbf{V}_{i,j_\mathsf{D}}^{E}||^2\Big)I_{N_2}, \tag{50}$$

to have its following minorant at $(V_\mathsf{D}^{(\kappa)}, V_\mathsf{U}^{(\kappa)}, \rho^{(\kappa)})$:

$$\Theta_i^{(\kappa)}(\mathbf{V}_\mathsf{D}, \mathbf{V}_\mathsf{U}, \boldsymbol{\rho}) \triangleq a_i^{(\kappa)} + 2\Re\left\{\langle\mathcal{A}_i^{(\kappa)}, \mathcal{L}_i(\mathbf{V}_{\mathsf{U}i})\rangle\right\} - \langle\mathcal{B}_i^{(\kappa)}, \mathcal{M}_i(\mathbf{V}_\mathsf{D}, \mathbf{V}_\mathsf{U}, \boldsymbol{\rho})\rangle, \tag{51}$$

where similarly to (21)

$$\begin{aligned} 0 > a_i^{(\kappa)} &= f_i(V_\mathsf{D}^{(\kappa)}, V_\mathsf{U}^{(\kappa)}) - \Re\left\{\langle\Psi_i^{-1}(V_\mathsf{D}^{(\kappa)}, V_\mathsf{U}^{(\kappa)})\mathcal{L}_i(V_i^{(\kappa)}), \mathcal{L}_i(V_i^{(\kappa)})\rangle\right\},\\ \mathcal{A}_i^{(\kappa)} &= \Psi_i^{-1}(V_\mathsf{D}^{(\kappa)}, V_\mathsf{U}^{(\kappa)})\mathcal{L}_i(V_{\mathsf{U}i}^{(\kappa)}),\\ 0 \preceq \mathcal{B}_i^{(\kappa)} &= \Psi_i^{-1}(V_\mathsf{D}^{(\kappa)}, V_\mathsf{U}^{(\kappa)}) - \mathcal{M}_i^{-1}(V_\mathsf{D}^{(\kappa)}, V_\mathsf{U}^{(\kappa)}). \end{aligned} \tag{52}$$

The function $\Theta_i^{(\kappa)}(\mathbf{V}_\mathsf{D}, \mathbf{V}_\mathsf{U}, \boldsymbol{\rho})$ is not concave due to the term $\bar{\Psi}_i^{TSI}(\mathbf{V}_\mathsf{D}, 1/\boldsymbol{\rho})$ defined by (50). However, the following matrix inequality holds:

$$\frac{1}{\boldsymbol{\rho}}||\mathbf{V}_{i,j_\mathsf{D}}^{E}||^2 I_{N_2} \succeq \Big(\frac{2}{\rho^{(\kappa)}}\Re\{\langle V_{i,j_\mathsf{D}}^{E,(\kappa)}, \mathbf{V}_{i,j_\mathsf{D}}^{E}\rangle\} - \frac{||V_{i,j_\mathsf{D}}^{E,(\kappa)}||^2}{(\rho^{(\kappa)})^2}\boldsymbol{\rho}\Big)I_{N_2}, \tag{53}$$

which yields the matrix inequality

$$\begin{aligned} &\mathcal{M}_i(\mathbf{V}_\mathsf{D}, \mathbf{V}_\mathsf{U}, \boldsymbol{\rho})\\ &\quad\geq \mathcal{M}_i^{(\kappa)}(\mathbf{V}_\mathsf{D}, \mathbf{V}_\mathsf{U}, \boldsymbol{\rho})\\ &\quad\triangleq (\mathcal{L}_i(\mathbf{V}_{\mathsf{U}i}))^2 + \bar{\Psi}_i^{U}(\mathbf{V}_\mathsf{U}) + \sigma_{SI}^2\Big(||\mathbf{V}_{i,j_\mathsf{D}}^{E}||^2 + \frac{1}{\boldsymbol{\rho}}||\mathbf{V}_{i,j_\mathsf{D}}^{I}||^2\\ &\qquad - \frac{2}{\rho^{(\kappa)}}\Re\{\langle V_{i,j_\mathsf{D}}^{E,(\kappa)}, \mathbf{V}_{i,j_\mathsf{D}}^{E}\rangle\} + \frac{||V_{i,j_\mathsf{D}}^{E,(\kappa)}||^2}{(\rho^{(\kappa)})^2}\boldsymbol{\rho}\Big)I_{N_2}. \end{aligned}$$

As $\mathcal{B}_i^{(\kappa)} \succeq 0$ by (52), we then have

$$\langle\mathcal{B}_i^{(\kappa)}, \mathcal{M}_i(\mathbf{V}_\mathsf{D}, \mathbf{V}_\mathsf{U}, \boldsymbol{\rho})\rangle \geq \langle\mathcal{B}_i^{(\kappa)}, \mathcal{M}_i^{(\kappa)}(\mathbf{V}_\mathsf{D}, \mathbf{V}_\mathsf{U}, \boldsymbol{\rho})\rangle$$

so a concave minorant of both $f_i(\mathbf{V}_\mathsf{D}, \mathbf{V}_\mathsf{U}, 1/\boldsymbol{\rho})$ and $\Theta^{(\kappa)}(\mathbf{V}_\mathsf{D}, \mathbf{V}_\mathsf{U}, \boldsymbol{\rho})$ is

$$\tilde{\Theta}_i^{(\kappa)}(\mathbf{V}_\mathsf{D}, \mathbf{V}_\mathsf{U}, \boldsymbol{\rho}) \triangleq a_i^{(\kappa)} + 2\Re\left\{\langle\mathcal{A}_i^{(\kappa)}, \mathcal{L}_i(\mathbf{V}_{\mathsf{U}_i})\rangle\right\} - \langle\mathcal{B}_i^{(\kappa)}, \mathcal{M}_i^{(\kappa)}(\mathbf{V}_\mathsf{D}, \mathbf{V}_\mathsf{U}, \boldsymbol{\rho})\rangle. \tag{54}$$

Concerned with $||\mathbf{V}_{i,j_\mathsf{D}}^{E}||^2/\boldsymbol{\rho}$ in the right hand side (RHS) of (41b) and (41c), it follows from (53) that

$$\begin{aligned} ||\mathbf{V}_{i,j_\mathsf{D}}^{E}||^2/\boldsymbol{\rho} &\geq \gamma_{i,j_\mathsf{D}}^{(\kappa)}(\mathbf{V}_{i,j_\mathsf{D}}^{E}, \boldsymbol{\rho})\\ &\triangleq 2\Re\Big\{\langle V_{i,j_\mathsf{D}}^{E,(\kappa)}, \mathbf{V}_{i,j_\mathsf{D}}^{E}\rangle\Big\}/\rho^{(\kappa)} - \boldsymbol{\rho}||V_{i,j_\mathsf{D}}^{E,(\kappa)}||^2/(\rho^{(\kappa)})^2. \end{aligned}$$

We also have $\phi_{i,j_\mathsf{D}}^{(\kappa)}(\mathbf{V}_\mathsf{D}^{E}, \mathbf{V}_\mathsf{U})$ defined in (22) as a minorant of $\langle\Phi_{i,j_\mathsf{D}}(\mathbf{V}_\mathsf{D}^{E}, \mathbf{V}_\mathsf{U})\rangle$. We now address the nonconvex problem (41) by successively solving its following innerly approximated convex program at the κ^{th} iteration:

$$\max_{\mathbf{V}_\mathsf{D}, \mathbf{V}_\mathsf{U}, \boldsymbol{\rho}>0} \mathcal{P}_2^{(\kappa)}(\mathbf{V}_\mathsf{D}, \mathbf{V}_\mathsf{U}, \boldsymbol{\rho}) \tag{55a}$$

$$\text{s.t. (40), (39c),} \tag{55b}$$

$$\sum_{(i,j_\mathsf{D})\in\mathcal{S}_1}\Big(||\mathbf{V}_{i,j_\mathsf{D}}^{E}||^2 + \frac{1}{\boldsymbol{\rho}}||\mathbf{V}_{i,j_\mathsf{D}}^{I}||^2\Big) + \sum_{(i,j_\mathsf{U})\in\mathcal{S}_2}||\mathbf{V}_{i,j_\mathsf{U}}||^2 \leq P + \sum_{(i,j_\mathsf{D})\in\mathcal{S}_1}\gamma_{i,j_\mathsf{D}}^{(\kappa)}(\mathbf{V}_{i,j_\mathsf{D}}^{E}, \boldsymbol{\rho}), \tag{55c}$$

$$\sum_{j_\mathsf{D}\in\mathcal{D}}\Big(||\mathbf{V}_{i,j_\mathsf{D}}^{E}||^2 + \frac{1}{\boldsymbol{\rho}}||\mathbf{V}_{i,j_\mathsf{D}}^{I}||^2\Big) \leq P_i + \sum_{j_\mathsf{D}\in\mathcal{D}}\gamma_{i,j_\mathsf{D}}^{(\kappa)}(\mathbf{V}_{i,j_\mathsf{D}}^{E}, \boldsymbol{\rho}), \forall i \in I, \tag{55d}$$

$$\phi_{i,j_\mathsf{D}}^{(\kappa)}(\mathbf{V}_\mathsf{D}^{E}, \mathbf{V}_\mathsf{U}) \geq e_{i,j_\mathsf{D}}^{\min}(1 + \frac{1}{\boldsymbol{\rho}-1})/\zeta_{i,j_\mathsf{D}},\ \forall(i, j_\mathsf{D}) \in \mathcal{S}_1, \tag{55e}$$

$$\tilde{\Theta}_i^{(\kappa)}(\mathbf{V}_\mathsf{D}, \mathbf{V}_\mathsf{U}, \boldsymbol{\rho}) \geq r_i^{\mathsf{U},\min}, \forall i \in I, \tag{55f}$$

$$g_{i,j_\mathsf{D}}^{(\kappa)}(\mathbf{V}_\mathsf{D}^{I}, \mathbf{V}_\mathsf{U}, \boldsymbol{\rho}) \geq r_{i,j_\mathsf{D}}^{\mathsf{D},\min}.\ \ \forall(i, j_\mathsf{D}) \in \mathcal{S}_1. \tag{55g}$$

where $\mathcal{P}_2^{(\kappa)}(\mathbf{V}_\mathsf{D}, \mathbf{V}_\mathsf{U}, \boldsymbol{\rho}) \triangleq \sum_{i\in I} \tilde{\Theta}_i^{(\kappa)}(\mathbf{V}_\mathsf{D}, \mathbf{V}_\mathsf{U}, \boldsymbol{\rho}) + \sum_{(i,j_\mathsf{D})\in\mathcal{S}_1} g_{i,j_\mathsf{D}}^{(\kappa)}(\mathbf{V}_\mathsf{D}^I, \mathbf{V}_\mathsf{U}, \boldsymbol{\rho})$.

A path-following procedure similar to Algorithm 1 can be applied to solve (41) as summarized in Algorithm 2. Thanks to the following relation, which is similar to (26):

$$\mathcal{P}_2(V_\mathsf{D}^{(\kappa+1)}, V_\mathsf{U}^{(\kappa+1)}, \rho^{(\kappa+1)}) \geq \mathcal{P}_2(V_\mathsf{D}^{(\kappa)}, V_\mathsf{U}^{(\kappa)}, \rho^{(\kappa)}), \quad (56)$$

Algorithm 2 improves upon the feasible point at each iteration and then converges to a local optimum after finitely many iterations.

Algorithm 2 Path-Following Algorithm for TS Optimization Problem (41)

Initialization: Set $\kappa := 0$, and choose a feasible point $(V_\mathsf{D}^{(0)}, V_\mathsf{U}^{(0)}, \alpha^{(0)})$ that satisfies (39b)-(39g). Set $\rho^{(0)} := 1/\alpha^{(0)}$.

κ-th iteration: Solve (55) for an optimal solution $(V_\mathsf{D}^*, V_\mathsf{U}^*, \rho^*)$, set $\kappa := \kappa + 1$, $(V_\mathsf{D}^{(\kappa)}, V_\mathsf{U}^{(\kappa)}, \rho^{(\kappa)}) := (V_\mathsf{D}^*, V_\mathsf{U}^*, \rho^*)$ and calculate $\mathcal{P}_2(V_\mathsf{D}^{(\kappa)}, V_\mathsf{U}^{(\kappa)}, 1/\rho^{(\kappa)})$. Stop if $\left|\left(\mathcal{P}_2(x^{(\kappa)}) - \mathcal{P}_2(x^{(\kappa-1)})\right)/\mathcal{P}_2(x^{(\kappa-1)})\right| \leq \epsilon$, where $x^{(\kappa)} \triangleq (V_\mathsf{D}^{(\kappa)}, V_\mathsf{U}^{(\kappa)}, 1/\rho^{(\kappa)})$.

To find an initial feasible point for Algorithm 2, we consider the following problem:

$$\max_{\mathbf{V}_\mathsf{D},\mathbf{V}_\mathsf{U},\boldsymbol{\rho}} \min_{(i,j_\mathsf{D})\in\mathcal{S}_1} \Big\{ f_i(\mathbf{V}_\mathsf{D}, \mathbf{V}_\mathsf{U}, 1/\boldsymbol{\rho}) - r_i^{\min}, \; E_{i,j_\mathsf{D}}(\mathbf{V}_\mathsf{D}^E, \mathbf{V}_\mathsf{U}, 1/\boldsymbol{\rho}) - e_{i,j_\mathsf{D}}^{\min}, \; f_{i,j_\mathsf{D}}(\mathbf{V}_\mathsf{D}^I, \mathbf{V}_\mathsf{U})/\boldsymbol{\rho} - r_{i,i_\mathsf{D}}^{\min} \Big\} : \; (41b) - (41c) \quad (57)$$

which can be addressed by successively solving the following convex maximin program:

$$\max_{\mathbf{V}_\mathsf{D},\mathbf{V}_\mathsf{U},\boldsymbol{\rho}} \min_{(i,j_\mathsf{D})\in\mathcal{S}_1} \Big\{ g_{i,j_\mathsf{D}}^{(\kappa)}(\mathbf{V}_\mathsf{D}^I, \mathbf{V}_\mathsf{U}, \boldsymbol{\rho}) - r_{i,i_\mathsf{D}}^{\min}, \; \phi_{i,j_\mathsf{D}}^{(\kappa)}(\mathbf{V}_\mathsf{D}^E, \mathbf{V}_\mathsf{U}) - e_{i,j_\mathsf{D}}^{\min}(1 + \frac{1}{\boldsymbol{\rho}-1})/\zeta_{i,j_\mathsf{D}}, \; \tilde{\Theta}_i^{(\kappa)}(\mathbf{V}_\mathsf{D}, \mathbf{V}_\mathsf{U}, \boldsymbol{\rho}) - r_i^{\min} \Big\} : \; (55b) - (55d), \quad (58)$$

upon reaching $f_{i,j_\mathsf{D}}(V_\mathsf{D}^{I,(\kappa)}, V_\mathsf{U}^{(\kappa)}, \alpha^{(\kappa)}) \geq r_{i,i_\mathsf{D}}^{\min}$, $f_i(V_\mathsf{D}^{(\kappa)}, V_\mathsf{U}^{(\kappa)}, \alpha^{(\kappa)}) \geq r_i^{\min}$ and $E_{i,j_\mathsf{D}}(V_\mathsf{D}^{E,(\kappa)}, V_\mathsf{U}^{(\kappa)}, 1/\rho^{(\kappa)}) \geq e_{i,j_\mathsf{D}}^{\min}$, $\forall (i, j_\mathsf{D}) \in \mathcal{S}_1$.

For the system operating in HD mode, we apply the same transmission strategy as in Section II. Specifically, we consider the following problem:

$$\max_{\mathbf{V}_\mathsf{D},\mathbf{V}_\mathsf{U},\boldsymbol{\rho}} \; \frac{1}{2}\Big[\sum_{(i,j_\mathsf{D})\in\mathcal{S}_1} \frac{1}{\boldsymbol{\rho}} f_{i,j_\mathsf{D}}(\mathbf{V}_\mathsf{D}, 0_\mathsf{U}) + \sum_{i\in I} f_i(0_\mathsf{D}, \mathbf{V}_\mathsf{U}, 1)\Big] \;\; \text{s.t. (39b)} - \text{(39e)} \quad (59a)$$

$$\frac{1}{2}(E_{i,j_\mathsf{D}}(\mathbf{V}_\mathsf{D}, 0_\mathsf{U}, 1/\boldsymbol{\rho}) + E_{i,j_\mathsf{D}}(0_\mathsf{D}, \mathbf{V}_\mathsf{U}, 1)), \geq e_{i,j_\mathsf{D}}^{\min} \; (i, j_\mathsf{D}) \in \mathcal{S}_1, \quad (59b)$$

$$\frac{1}{2\boldsymbol{\rho}} f_{i,j_\mathsf{D}}(\mathbf{V}_\mathsf{D}, 0_\mathsf{U}) \geq r_{i,j_\mathsf{D}}^{\mathsf{D},\min}, \forall (i, j_\mathsf{D}) \in \mathcal{S}_1, \quad (59c)$$

$$\frac{1}{2} f_i(0_\mathsf{D}, \mathbf{V}_\mathsf{U}, 1) \geq r_i^{\mathsf{U},\min}, \quad \forall i \in I. \quad (59d)$$

In (59), DLUs harvest energy for a fraction $(1-\boldsymbol{\alpha})$ of $1/2$ of a time slot during DL transmission and for the whole $1/2$ time slot during UL transmission as formulated in (59b). The constraint (59b) can be written as

$$\Xi_{i,j_\mathsf{D}}(\mathbf{V}_\mathsf{D}, \mathbf{V}_\mathsf{U}, \boldsymbol{\rho}) \geq \frac{2e_{i,j_\mathsf{D}}^{\min}}{\zeta_{i,j_\mathsf{D}}} \left(1 + \frac{1}{\boldsymbol{\rho}-1}\right), \quad (60)$$

for

$$\Xi_{i,j_\mathsf{D}}(\mathbf{V}_\mathsf{D}, \mathbf{V}_\mathsf{U}, \boldsymbol{\rho}) \triangleq \langle \Phi_{i,j_\mathsf{D}}(\mathbf{V}_\mathsf{D}, 0_\mathsf{U})\rangle + \langle \Phi_{i,j_\mathsf{D}}(0_\mathsf{D}, \mathbf{V}_\mathsf{U})\rangle + \frac{\langle \Phi_{i,j_\mathsf{D}}(0_\mathsf{D}, \mathbf{V}_\mathsf{U})\rangle}{\boldsymbol{\rho}-1}.$$

As Ξ_{i,j_D} is convex, its minorant is its first-order approximation at $(V_\mathsf{D}^{(\kappa)}, V_\mathsf{U}^{(\kappa)}, \rho^{(\kappa)})$:

$$\Xi_{i,j_\mathsf{D}}^{(\kappa)}(\mathbf{V}_\mathsf{D}, \mathbf{V}_\mathsf{U}, \boldsymbol{\rho}) = \phi_{i,j_\mathsf{D}}^{(\kappa)}(\mathbf{V}_\mathsf{D}, 0_\mathsf{U}) + \phi_{i,j_\mathsf{D}}^{(\kappa)}(0_\mathsf{D}, \mathbf{V}_\mathsf{U}) + \Lambda_{i,j_\mathsf{D}}^{(\kappa)}(\mathbf{V}_\mathsf{U}, \boldsymbol{\rho} - 1),$$

for $\Lambda_{i,j_\mathsf{D}}^{(\kappa)}(\cdot,\cdot)$ defined by (31) and $\phi_{i,j_\mathsf{D}}^{(\kappa)}(0_\mathsf{D}, \mathbf{V}_\mathsf{U})$ defined from (22) with both $\mathbf{V}_\mathsf{U}$ and $V_\mathsf{U}^{(\kappa)}$ replaced by 0_U.

The problem (39) thus can be addressed via a path-following procedure similar to Algorithm 2 where the following convex program is solved at the κ^{th} iteration:

$$\max_{\mathbf{V}_\mathsf{D},\mathbf{V}_\mathsf{U},\boldsymbol{\rho}} \; \frac{1}{2}\Big[\sum_{(i,j_\mathsf{D})\in\mathcal{S}_1} g_{i,j_\mathsf{D}}^{(\kappa)}(\mathbf{V}_\mathsf{D}^I, 0_\mathsf{U}, \boldsymbol{\rho}) + \sum_{i\in I} \tilde{\Theta}_i^{(\kappa)}(0_\mathsf{D}, \mathbf{V}_\mathsf{U}, 1)\Big] : \text{(39b)} - \text{(39e)} \quad (61a)$$

$$\Xi_{i,j_\mathsf{D}}^{(\kappa)}(\mathbf{V}_\mathsf{D}, \mathbf{V}_\mathsf{U}, \boldsymbol{\rho}) \geq \frac{2e_{i,j_\mathsf{D}}^{\min}}{\zeta_{i,j_\mathsf{D}}}(1 + \frac{1}{\boldsymbol{\rho}-1}), \; (i, j_\mathsf{D}) \in \mathcal{S}_1, \quad (61b)$$

$$\frac{1}{2} g_{i,j_\mathsf{D}}^{(\kappa)}(\mathbf{V}_\mathsf{D}, 0_\mathsf{U}, \boldsymbol{\rho}) \geq r_{i,j_\mathsf{D}}^{\mathsf{D},\min}, \quad \forall (i, j_\mathsf{D}) \in \mathcal{S}_1, \quad (61c)$$

$$\frac{1}{2} \tilde{\Theta}_i^{(\kappa)}(0_\mathsf{D}, \mathbf{V}_\mathsf{U}, 1) \geq r_i^{\mathsf{U},\min}, \quad \forall i \in I, \quad (61d)$$

where $g_{i,j_\mathsf{D}}^{(\kappa)}(\mathbf{V}_\mathsf{D}^I, 0_\mathsf{U}, \boldsymbol{\rho})$ is defined by (48) with both $\mathbf{V}_\mathsf{U}$ and $V_\mathsf{U}^{(\kappa)}$ replaced by 0_U, while $\tilde{\Theta}_i^{(\kappa)}(0_\mathsf{D}, \mathbf{V}_\mathsf{U}, 0)$ is defined by (54) with both $\mathbf{V}_\mathsf{D}$ and $V_\mathsf{D}^{(\kappa)}$ replaced by 0_D and both $\boldsymbol{\rho}$ and $\rho^{(\kappa)}$ replaced by 1.

IV. Throughput QoS Constrained Energy-Harvesting Optimization

We will justify numerically that TS is not only easier to implement but performs better than PS for FD EH-enabled MU MIMO networks. This motivates us to consider the following EH optimization with TS, which has not been considered previously:

$$\max_{\mathbf{V}_\mathsf{D},\mathbf{V}_\mathsf{U},\boldsymbol{\alpha}} \mathcal{P}_3(\mathbf{V}, \boldsymbol{\alpha}) \triangleq \sum_{(i,j_\mathsf{D})\in\mathcal{S}_1} E_{i,j_\mathsf{D}}(\mathbf{V}_\mathsf{D}^E, \mathbf{V}_\mathsf{U}, \boldsymbol{\alpha}) \quad \text{s.t. (39b)} - \text{(39g)}. \quad (62)$$

By defining $\boldsymbol{\rho} = 1/\boldsymbol{\alpha}$, we firstly recast $E_{i,j_\mathsf{D}}(\mathbf{V}_\mathsf{D}^E, \mathbf{V}_\mathsf{U}, 1/\boldsymbol{\rho})$ as

$$E_{i,j_\mathsf{D}}(\mathbf{V}_\mathsf{D}^E, \mathbf{V}_\mathsf{U}, 1/\boldsymbol{\rho}) = \zeta_{i,j_\mathsf{D}}\Big(\langle \Phi_{i,j_\mathsf{D}}(\mathbf{V}_\mathsf{D}^E, \mathbf{V}_\mathsf{U})\rangle - Q_{i,j_\mathsf{D}}(\mathbf{V}_\mathsf{D}^E, \mathbf{V}_\mathsf{U}, \boldsymbol{\rho})\Big), \quad (63)$$

where $Q_{i,j_\mathsf{D}}(\mathbf{V}_\mathsf{D}^E, \mathbf{V}_\mathsf{U}, \boldsymbol{\rho}) \triangleq \frac{1}{\boldsymbol{\rho}}\langle \Phi_{i,j_\mathsf{D}}(\mathbf{V}_\mathsf{D}^E, \mathbf{V}_\mathsf{U})\rangle$ is a convex function. Recalling that $\phi_{i,j_\mathsf{D}}^{(\kappa)}(\mathbf{V}_\mathsf{D}^E, \mathbf{V}_\mathsf{U})$ defined in (22) is a minorant of $\langle \Phi_{i,j_\mathsf{D}}(\mathbf{V}_\mathsf{D}^E, \mathbf{V}_\mathsf{U})\rangle$, we can now address the non-convex problem (62) by successively solving the following convex program at the κ^{th} iteration:

$$\begin{aligned}\max_{\mathbf{V},\boldsymbol{\rho}} \sum_{(i,j_\mathsf{D})\in\mathcal{S}_1} \zeta_{i,j_\mathsf{D}} \Big(&\phi_{i,j_\mathsf{D}}^{(\kappa)}(\mathbf{V}_\mathsf{D}^E, \mathbf{V}_\mathsf{U}) \\ &- Q_{i,j_\mathsf{D}}(\mathbf{V}_\mathsf{D}^E, \mathbf{V}_\mathsf{U}, \boldsymbol{\rho})\Big) \\ \text{s.t. } &(39\text{c}), (40), (55\text{c}), (55\text{d}), (55\text{f}), (55\text{g}). \end{aligned} \tag{64}$$

A path-following procedure similar to Algorithm 2 can be applied to solve (62).

For the system operating in HD mode, the same transmission strategy as in Section II is applied. Specifically, we consider the following problem:

$$\begin{aligned}\max_{\mathbf{V},\boldsymbol{\rho}} \sum_{(i,j_\mathsf{D})\in\mathcal{S}_1} &\frac{1}{2}(E_{i,j_\mathsf{D}}(\mathbf{V}_\mathsf{D}^E, 0_\mathsf{U}, 1/\boldsymbol{\rho}) + E_{i,j_\mathsf{D}}(0_\mathsf{D}, \mathbf{V}_\mathsf{U}, 0)) \\ \text{s.t. } &(39c), (40), (39d), (39e), (59c), (59d). \end{aligned} \tag{65}$$

The problem (65) can be addressed via a path-following procedure similar to Algorithm 2 where the following convex program is solved at the κ^{th} iteration:

$$\begin{aligned}\max_{\mathbf{V},\boldsymbol{\rho}} \sum_{(i,j_\mathsf{D})\in\mathcal{S}_1} &\frac{\zeta_{i,j_\mathsf{D}}}{2}\Big(\phi_{i,j_\mathsf{D}}^{(\kappa)}(\mathbf{V}_\mathsf{D}^E, 0_\mathsf{U}) - Q_{i,j_\mathsf{D}}(\mathbf{V}_\mathsf{D}^E, 0_\mathsf{U}, \boldsymbol{\rho}) \\ &+ \phi_{i,j_\mathsf{D}}^{(\kappa)}(0_\mathsf{D}, \mathbf{V}_\mathsf{U})\Big) \\ \text{s.t. } &(39c), (40), (39d), (39e), (61c), (61d), \end{aligned} \tag{66}$$

where $\phi_{i,j_\mathsf{D}}^{(\kappa)}(\mathbf{V}_\mathsf{D}^E, 0_\mathsf{U})$ ($\phi_{i,j_\mathsf{D}}^{(\kappa)}(0_\mathsf{D}, \mathbf{V}_\mathsf{U})$, resp.) is defined by (22) with both $\mathbf{V}_\mathsf{U}$ and $V_\mathsf{U}^{(\kappa)}$ (both $\mathbf{V}_\mathsf{D}$ and $V_\mathsf{D}^{(\kappa)}$, resp.) replaced by 0_U (0_D, resp.).

Problems (55), (58), (61), (64) and (66) involve $n = 2(N_1 d_1 ID + N_r d_2 IU) + 3$ scalar real decision variables and $m = ID + IU + 2I + 3$ quadratic constraints so their computational complexity is $O(n^2 m^{2.5} + m^{3.5})$.

V. Numerical Results

In this simulation study, we use the example network in Fig. 2 to study the total network throughput in the presence of SI. The HD system is also implemented as a baseline for both time splitting and power splitting cases. DLUs are randomly located on the circles with radii $r_1 = 20$ m centered at their serving BSs whereas ULUs are uniformly distributed within the cell of their serving BSs whose radii are $r_2 = 40$ m. There are two DLUs and two ULUs within each cell. We set the path loss exponent $\beta = 4$. For small-scale fading, we generate the channel matrices H_{m,i,j_D} from BS m to UE (i, j_D), matrices $H_{i,j_\mathsf{D},\ell_\mathsf{U}}$ from ULU (i, ℓ_U) to DLU (i, j_D), matrices $H_{m,\ell_\mathsf{U},i}$ from ULU (m, ℓ_U) to BS i and matrices $H_{m,i}^{\mathcal{B}}$ from BS m to BS i using the Rician fading model as follows:

$$H = \sqrt{\frac{K_R}{1+K_R}} H^{LOS} + \sqrt{\frac{1}{1+K_R}} H^{NLOS}, \tag{67}$$

where $K_R = 10$ dB is the Rician factor, H^{LOS} is the line-of-sight (LOS) deterministic component and each element of the Rayleigh fading component H^{NLOS} is a circularly-symmetric complex Gaussian random variable $\mathcal{CN}(0, 1)$. Here, we use the far-field uniform linear antenna array model [32] with

$$\begin{aligned} H^{LOS} = &[1, e^{j\theta_r}, e^{j2\theta_r}, \ldots, e^{j(N_r-1)\theta_r}] \\ &\times [1, e^{j\theta_t}, e^{j2\theta_t}, \ldots, e^{j(N_1-1)\theta_t}]^H, \end{aligned} \tag{68}$$

for $\theta_r = \frac{2\pi d \sin(\phi_r)}{\lambda}$, $\theta_t = \frac{2\pi d \sin(\phi_t)}{\lambda}$, where $d = \lambda/2$ is the antenna spacing, λ is the carrier wavelength, and ϕ_r and ϕ_t are the angle-of-arrival and angle-of-departure, respectively. In our simulations, ϕ_r and ϕ_t are randomly generated between 0 and 2π. Unless stated otherwise, the number of transmit antennas and the number of receive antennas at a BS are set as $N_1 = N_2 = 4$. The numbers of concurrent downlink data streams and the numbers of concurrent uplink data streams are equal and $d_1 = d_2 = N_r$. To arrive at the final figures, we run each simulation 100 times and average over the results. In all simulations, we set $P = 23$ dBW, $P_i = 16$ dBW $\forall i \in I$, $P_{i,j_\mathsf{U}} = 10$ dBW $\forall (i, j_\mathsf{U}) \in \mathcal{S}_2$, $\forall i \in I$,$\zeta = 0.5$, $\sigma_c^2 = -90$ dBW, $\sigma^2 = -90$ dBW, $r_{i,j_\mathsf{D}}^{\min} = r^\mathsf{D} = 1$ bps/Hz and $r_i^{\min} = r^\mathsf{U} = Ur^\mathsf{D}$ bps/Hz. We further assume that the required harvested energies of all DLUs are the same and $e_{i,j_\mathsf{D}}^{\min} = e^{\min}$, $\forall (i, j_\mathsf{D})$. Unless stated otherwise, we set $e^{\min} = -20$ dBm as in [7] and [33]. According to the current state-of-the-art-electronic circuitry, the sensitivity level of a typical energy harvester is around -20 dBm (0.01mW) [33], which means that we can activate the EH circuitry with that much received power. The SI level σ_{SI}^2 is choosen within the range $[-150, -90]$ dB[1] as in [14], [16], and [26], where $\sigma_{SI}^2 = -150$ dB represents almost perfect SI cancellation.

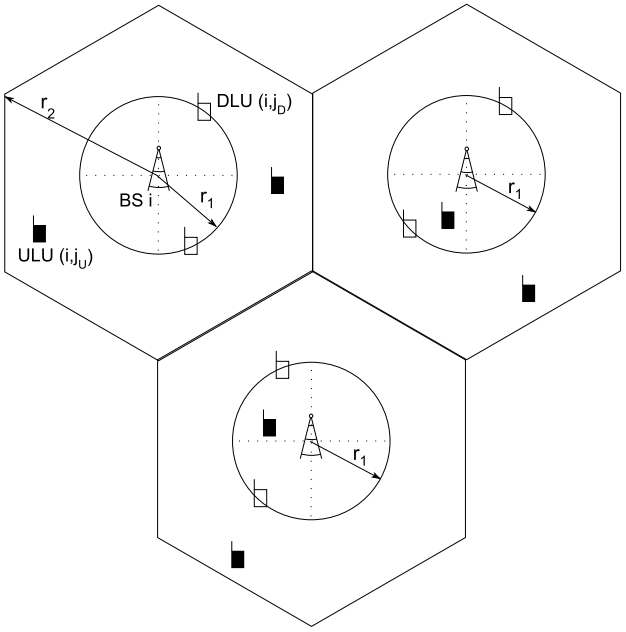

Fig. 2. A three-cell network with three DLUs and three ULUs. DLUs are randomly located on the circles with radii r_1 centered at their serving BSs. ULUs are uniformly distributed within the cell of their serving BSs.

[1]At $\sigma_{SI}^2 = -90$ dB, if a BS transmits at full power (i.e. 16 dBW), the SI power is 16 dB stronger than the background AWGN.

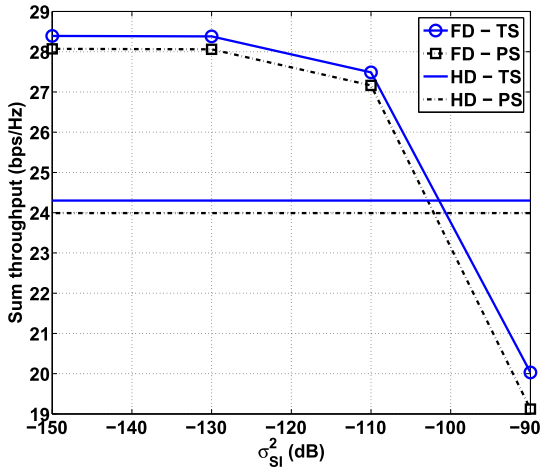

(a) $N_r = 1$

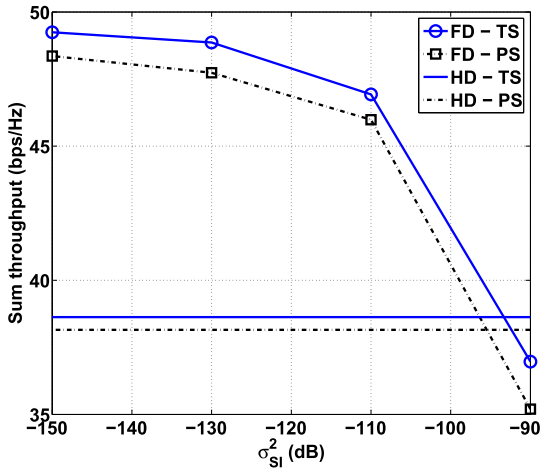

(b) $N_r = 2$

Fig. 3. Effect of SI on the sum throughput performance in the single-cell networks.

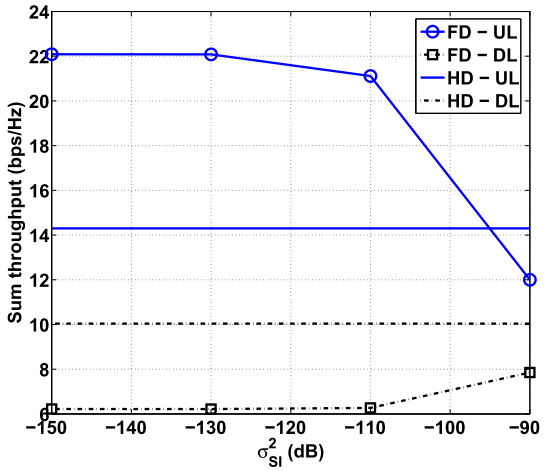

(a) $N_r = 1$

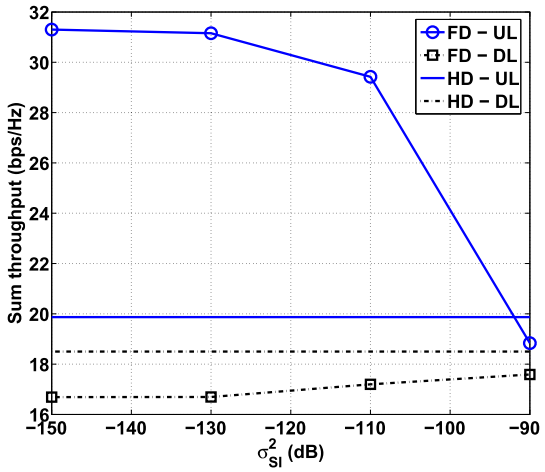

(b) $N_r = 2$

Fig. 4. Effect of SI on the UL/DL throughput performance in the single-cell networks.

A. Single Cell Network

Firstly, we consider the sum throughput maximization problem and the total harvested energy in the single cell networks. This will facilitate the analysis of the impact of SI on the network performance since there is no intercell interference. The network setting in Fig. 2 is used but only one cell is considered.

Fig. 3 illustrates the comparison of total network throughput between the power splitting mechanism and the time splitting mechanism in both FD and HD systems. Though FD provides a substantial improvement in comparison to HD in both power splitting (25.8%) and time splitting (26.1%) systems for $N_r = 2$ [2] at $\sigma^2_{SI} = -150$ dB, we cannot expect an FD system to achieve twice the throughput of an HD system. This is because even when the SI cancellation is perfect, DLUs in FD are still vulnerable to the intracell interference from the ULUs of the same cell. Moreover, DLUs and ULUs in HD are served with more BS antennas, resulting in a larger spatial diversity. Consequently, FD cannot double HD's throughput even with almost perfect SI cancellation.

When we reduce the number of antennas at UEs from $N_r = 2$ to $N_r = 1$, the total network throughput of FD is significantly reduced, by 42% for time splitting and by 41% for power splitting at $\sigma^2_{SI} = -150$ dB. Notably, since the UEs in FD are exposed to more sources of interference than UEs in HD, reducing the number of antennas of the UEs degrades the performance of FD more than the counterpart of HD. Consequently, the improvement of FD in comparison to HD reduces to 16% at $\sigma^2_{SI} = -150$ dB for both time splitting and power splitting.

Fig. 4 further illustrates how the total throughput is distributed into the downlink and uplink channels in the time splitting case. The behavior of the power splitting mechanism is similar and omitted here for brevity. With increasing σ^2_{SI}, the UL throughput consistently decreases. Moreover, since the UL transmission becomes less efficient, ULUs reduce their transmission power to reduce the interference toward

[2] N_r has been defined in the begining of Section II as the number of antennas of the UEs (DLUs and ULUs).

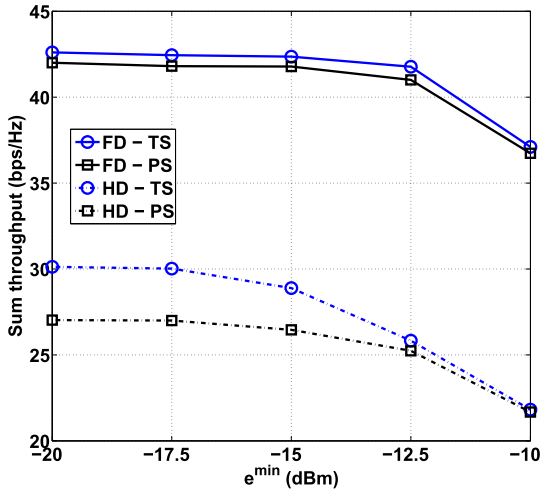

(a) $P_i = 30$ dBm

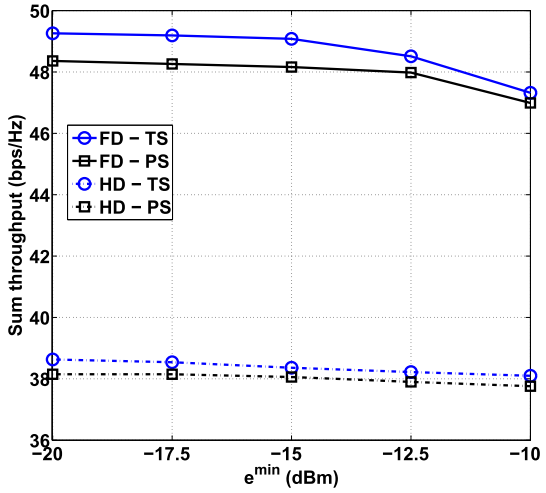

(b) $P_i = 46$ dBm

Fig. 5. Effect of energy harvesting constraints on the total harvested energy performance in the single-cell networks.

DLUs. Consequently, a slight increase in FD DL throughput is observed as σ_{SI}^2 increases. Another note is that since the distance between ULU-DLU in a small cell can be quite small due to the random deployment of ULUs and DLUs, DLUs' throughput can be severely degraded by the interference from ULUs. In fact, the FD DL throughput is 60% less than the counterpart of HD at $N_r = 1$ and $\sigma_{SI}^2 = -150$ dB. By using multiple antennas at the UEs (i.e. $N_r = 2$), the DLUs in FD can handle the interference better and the FD DL throughput at $\sigma_{SI}^2 = -150$ dB is only 10% less than the counterpart of HD.

To analyze the effect of the energy harvesting constraint, we fix $N_r = 2, \sigma_{SI}^2 = -110$ dB and vary $e^{\min}$. Fig. 5 illustrates a consistent decreasing trend of all schemes as $e^{\min}$ increases. The time splitting scheme outperforms the power splitting scheme in the considered range of $e^{\min}$ for both FD and HD. A similar conclusion can be drawn from Fig. 3. By using two different precoder matrices $\mathbf{V}^I$ and $\mathbf{V}^E$ for data transmission and energy transfer, the time splitting scheme can exploit the spatial diversity better than the power splitting scheme which only uses one type of precoder matrix for both purposes. Thus, the time splitting scheme is more efficient than the power splitting scheme in terms of performance.

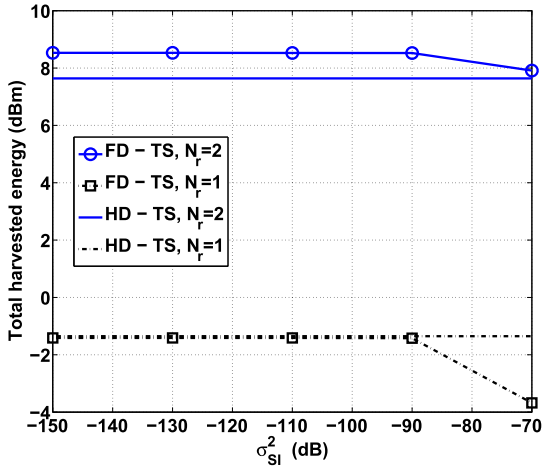

Fig. 6. Effect of SI on the total harvested energy performance in the single-cell networks.

A comparison of the maximum harvested energy of the time splitting scheme in both FD and HD systems is presented in Fig. 6. Interestingly, in the case $N_r = 1$, FD roughly harvests as much as HD. The reason for this is twofold. Firstly, it has been reported in [16], [26], and [34] that FD does not always harness performance gain over HD if the distances between ULUs and DLUs are not large enough. Since we consider small cell networks with randomly deployed ULUs and DLUs, the ULU-DLU distance can be very small, which creates significant interference to DLUs. Secondly, with $N_r = 1$, DLUs cannot exploit spatial diversity to mitigate the interference from ULUs. Consequently, ULUs must reduce their transmit power to ensure the QoS at the DLUs, which lowers the amount of harvested energy at the DLUs. In contrast, the results show that FD harvests more energy than HD given that $\sigma_{SI}^2 \leq -90$ dB for $N_r = 2$. All this implies that having multiple antennas at UEs is important to combat the extra interference in FD.

B. Three-Cell Network

Now, we consider the sum throughput maximization problem and the total harvested energy in the three-cell network depicted in Fig. 2. In this scenario, the DLUs and BSs are exposed to additional intercell interference. According to Fig. 7, FD now only provides a marginal improvement over HD for both power splitting (11.7%) and time splitting (11.8%) for $N_r = 2$ and $\sigma_{SI}^2 = -150$ dB. For $N_r = 1$ and $\sigma_{SI}^2 = -150$ dB, the improvement is even lower with 4.1% for power splitting and 4.4% for time splitting. Therefore, FD can give marginal gains compared to HD in multi-cell networks with high levels of interference.

The effect of the energy harvesting constraint on the network sum throughput is also investigated in Fig. 8 for the three-cell networks with $N_r = 2$ and $\sigma_{SI}^2 = -110$ dB. As in

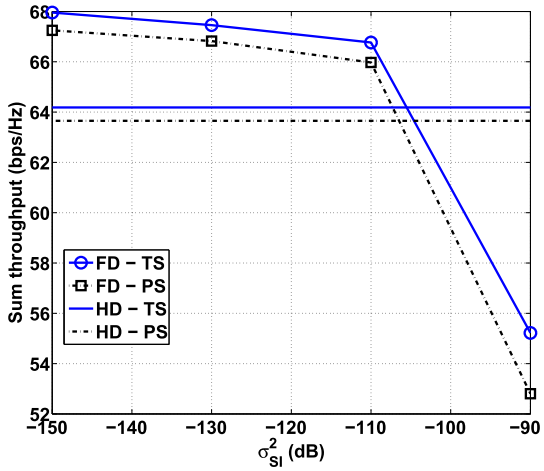

(a) $N_r = 1$

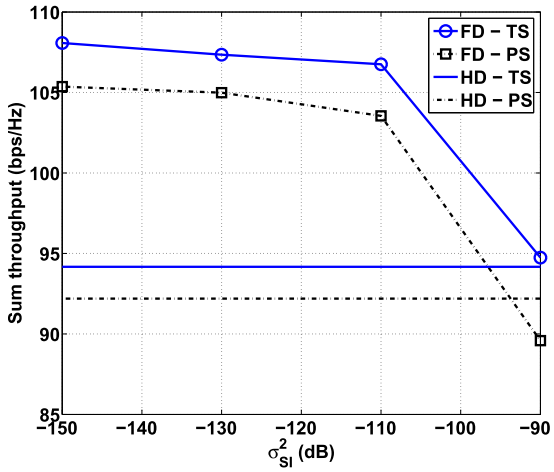

(b) $N_r = 2$

Fig. 7. Effect of SI on the sum throughput performance in the three-cell networks.

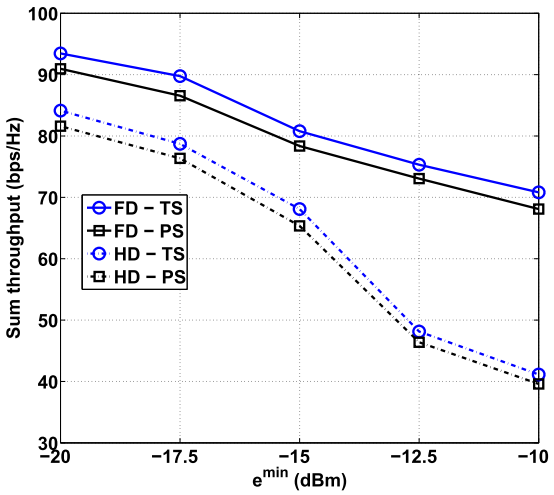

(a) $P_i = 30$ dBm

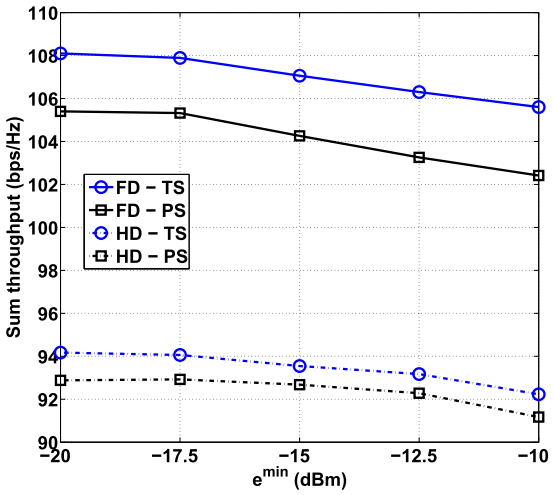

(b) $P_i = 46$ dBm

Fig. 8. Effect of energy harvesting constraints on the total harvested energy performance in the three-cell networks.

Fig. 5, a consistent decreasing trend of all schemes is observed as $e^{\min}$ increases. Since DLUs can also harvest energy from the signals arriving from other BSs in multicell networks, the FD network throughput only decreases by about 3% for both harvesting schemes when $e^{\min}$ increases from -20 dBm to -10 dBm. The counterpart throughput decrease in single-cell scenarios was about 8%.

Fig. 9 also provides a comparison of the total harvested energy per cell of the EH maximization problem in both FD and HD systems in the three-cell network. For $N_r = 1$, FD even harvests less energy than HD given $\sigma^2_{SI} > -150$ dB due to the increasing level of interference when compared to a single-cell network. Similar to the single-cell network, FD outperforms HD for $\sigma^2_{SI} \leq -90$ dB if more antennas are deployed at the UEs (i.e. $N_r = 2$). This observation again emphasizes the importance of having multiple antennas at the UEs in FD to mitigate interference. Another note is that given $N_r = 2$ the amount of energy harvested per cell in three-cell networks (i.e. 10.09 dBm at $\sigma^2_{SI} = -150$ dB) is much higher than the harvested energy of the single cell in Fig. 6 (i.e. 8.5 dBm at $\sigma^2_{SI} = -150$ dB), thanks to the extra energy harvested from the intercell interference.

C. Convergence Behavior

Finally, the convergence behavior of the proposed Algorithm 1 is illustrated in Fig. 10. For brevity, we only present the case of the three-cell network at $\sigma^2_{SI} = -110$ dB and $N_r = 2$. Fig. 10(a) plots the convergence of the objective functions of the sum throughput maximization problem for the time splitting scheme and the power splitting scheme, whereas Fig. 10(b) plots the convergence of the objective function of the EH maximization problem. As can be seen, the sum throughput maximization problem achieve 90% of its final optimal value within 40 iterations whereas the EH maximization problem needs 10 iterations. Table I shows the average number of iterations required to solve each program. Note that each iteration of the proposed algorithms invokes a convex subproblem to generate a new feasible point

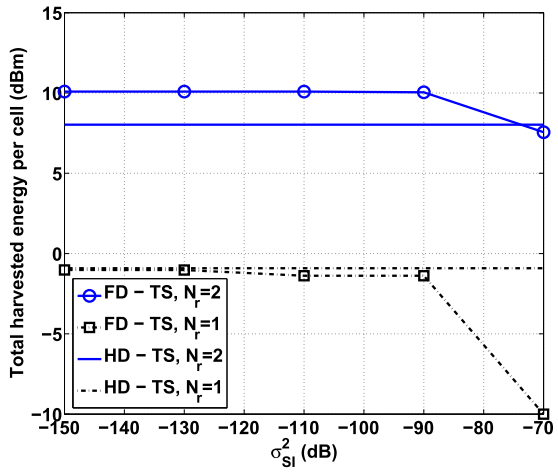

Fig. 9. Effect of SI on the total harvested energy performance in the three-cell networks.

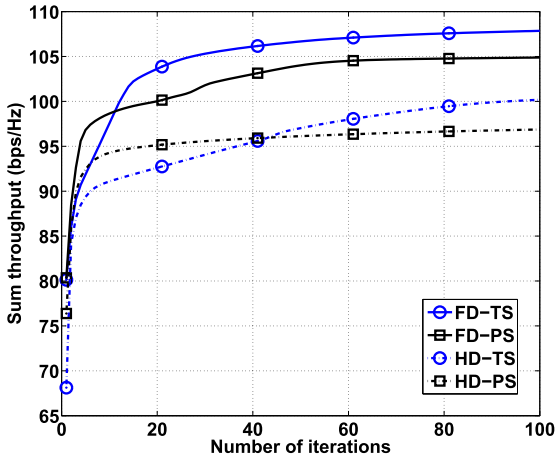

(a) Sum throughput maximization

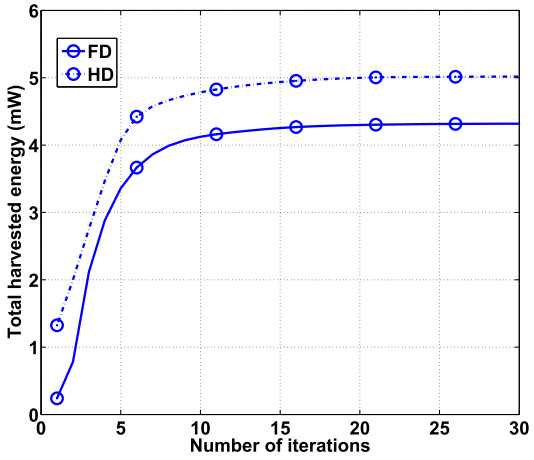

(b) EH maximization

Fig. 10. Convergence of the proposed algorithms for $\epsilon = 10^{-4}$.

$(V_{\mathsf{D}}^{(\kappa+1)}, V_{\mathsf{U}}^{(\kappa+1)}, \alpha^{(\kappa+1)})$ that is better than the incumbent $(V_{\mathsf{D}}^{(\kappa)}, V_{\mathsf{U}}^{(\kappa)}, \alpha^{(\kappa)})$. Such a convex subproblem can be solved efficiently by the available convex solvers of polynomial complexity such as CVX [35]. To save the computational time, it is recommended to input the incumbent $(V_{\mathsf{D}}^{(\kappa)}, V_{\mathsf{U}}^{(\kappa)}, \alpha^{(\kappa)})$ as the initial point for the process of solving this subproblem. Also, the high dimensionality and the nonconvexity of the considered problems imply that checking the global optimality of the computed solution is both theoretically and practically prohibitive. Nevertheless, our recent results in [9] and [10] for the particular MISO case of the HD optimization problem (29) show that both Algorithm 1 and Algorithm 2 are capable of delivering the globally optimal solutions.

TABLE I

THE AVERAGE NUMBER OF ITERATIONS REQUIRED BY THE PROPOSED ALGORITHMS

Programs	Throughput max., TS	Throughput max., PS	EH max.
FD	74	65.4	24.1
HD	67.5	50.6	20.2

VI. CONCLUSION

We have proposed new optimal precoding designs for EH-enabled FD multicell MU-MIMO networks. Specifically, sum throughput maximization under throughput QoS constraints and EH constraints for energy-constrained devices under either TS or PS has been considered. The FD EH maximization problem under throughput QoS constraints in TS has also been addressed. Toward this end, we have developed new path-following algorithms for their solution, which require a convex quadratic program for each iteration and are guaranteed to monotonically converge at least to a local optimum. Finally, we have demonstrated the merits of our proposed algorithms through extensive simulations. Note that an interesting topic for further research is this area is robust precoder/beamformer design in the presence of channel estimation errors.

REFERENCES

[1] X. Lu, D. Niyato, P. Wang, D. I. Kim, and Z. Han, "Wireless charger networking for mobile devices: Fundamentals, standards, and applications," *IEEE Wireless Commun.*, vol. 22, no. 2, pp. 126–135, Apr. 2015.

[2] X. Lu, P. Wang, D. Niyato, D. I. Kim, and Z. Han, "Wireless charging technologies: Fundamentals, standards, and network applications," *IEEE Commun. Surveys Tuts.*, vol. 18, no. 2, pp. 1413–1452, 2nd Quart., 2016.

[3] S. Buzzi, C. L. I, T. E. Klein, H. V. Poor, C. Yang, and A. Zappone, "A survey of energy-efficient techniques for 5G networks and challenges ahead," *IEEE J. Sel. Areas Commun.*, vol. 34, no. 4, pp. 697–709, Apr. 2016.

[4] J. G. Andrews *et al.*, "What will 5G be?" *IEEE J. Sel. Areas Commun.*, vol. 32, no. 6, pp. 1065–1082, Jun. 2014.

[5] Z. Ding *et al.*, "Application of smart antenna technologies in simultaneous wireless information and power transfer," *IEEE Commun. Mag.*, vol. 53, no. 4, pp. 86–93, Apr. 2015.

[6] S. Timotheou, I. Krikidis, G. Zheng, and B. Ottersten, "Beamforming for MISO interference channels with QoS and RF energy transfer," *IEEE Trans. Wireless Commun.*, vol. 13, no. 5, pp. 2646–2658, May 2014.

[7] Q. Shi, W. Xu, T. H. Chang, Y. Wang, and E. Song, "Joint beamforming and power splitting for MISO interference channel with SWIPT: An SOCP relaxation and decentralized algorithm," *IEEE Trans. Signal Process.*, vol. 62, no. 23, pp. 6194–6208, Dec. 2014.

[8] A. A. Nasir, D. T. Ngo, H. D. Tuan, and S. Durrani, "Iterative optimization for max-min SINR in dense small-cell multiuser MISO SWIPT system," in *Proc. IEEE Global Conf. Signal Process. (GlobalSIP)*, Dec. 2015, pp. 1392–1396.

[9] A. A. Nasir, H. D. Tuan, D. T. Ngo, S. Durrani, and D. I. Kim, "Path-following algorithms for beamforming and signal splitting in RF energy harvesting networks," *IEEE Commun. Lett.*, vol. 20, no. 8, pp. 1687–1690, Aug. 2016.
[10] A. A. Nasir, H. D. Tuan, D. T. Ngo, T. Q. Duong, and H. V. Poor, "Beamforming design for wireless information and power transfer systems: Receive power-splitting versus transmit time-switching," *IEEE Trans. Commun.*, vol. 65, no. 2, pp. 876–889, Feb. 2017.
[11] J. Park and B. Clerckx, "Joint wireless information and energy transfer in a K-user MIMO interference channel," *IEEE Trans. Wireless Commun.*, vol. 13, no. 10, pp. 5781–5796, Oct. 2014.
[12] J. Park and B. Clerckx, "Joint wireless information and energy transfer with reduced feedback in MIMO interference channels," *IEEE J. Sel. Areas Commun.*, vol. 33, no. 8, pp. 1563–1577, Aug. 2015.
[13] R. Zhang and C. K. Ho, "MIMO broadcasting for simultaneous wireless information and power transfer," *IEEE Trans. Wireless Commun.*, vol. 12, no. 5, pp. 1989–2001, May 2013.
[14] D. Nguyen, L.-N. Tran, P. Pirinen, and M. Latva-Aho, "Precoding for full duplex multiuser MIMO systems: Spectral and energy efficiency maximization," *IEEE Trans. Signal Process.*, vol. 61, no. 16, pp. 4038–4050, Aug. 2013.
[15] Z. Zong, H. Feng, F. R. Yu, N. Zhao, T. Yang, and B. Hu, "Optimal transceiver design for SWIPT in K-user MIMO interference channels," *IEEE Trans. Wireless Commun.*, vol. 15, no. 1, pp. 430–445, Jan. 2016.
[16] H. H. M. Tam, H. D. Tuan, and D. T. Ngo, "Successive convex quadratic programming for quality-of-service management in full-duplex MU-MIMO multicell networks," *IEEE Trans. Commun.*, vol. 64, no. 6, pp. 2340–2353, Jun. 2016.
[17] E. Everett, A. Sahai, and A. Sabharwal, "Passive self-interference suppression for full-duplex infrastructure nodes," *IEEE Trans. Wireless Commun.*, vol. 13, no. 2, pp. 680–694, Jan. 2014.
[18] M. Duarte *et al.*, "Design and characterization of a full-duplex multiantenna system for WiFi networks," *IEEE Trans. Veh. Technol.*, vol. 63, no. 3, pp. 1160–1177, Mar. 2014.
[19] L. Anttila, D. Korpi, E. Antonio-Rodríguez, R. Wichman, and M. Valkama, "Modeling and efficient cancellation of nonlinear self-interference in MIMO full-duplex transceivers," in *Proc. IEEE Global Commun. Conf. (Globecom)*, Dec. 2014, pp. 777–783.
[20] M. Heino *et al.*, "Recent advances in antenna design and interference cancellation algorithms for in-band full duplex relays," *IEEE Commun. Mag.*, vol. 53, no. 5, pp. 91–101, May 2015.
[21] M. Duarte, C. Dick, and A. Sabharwal, "Experiment-driven characterization of full-duplex wireless systems," *IEEE Trans. Wireless Commun.*, vol. 11, no. 12, pp. 4296–4307, Dec. 2012.
[22] Y.-S. Choi and H. Shirani-Mehr, "Simultaneous transmission and reception: Algorithm, design and system level performance," *IEEE Trans. Wireless Commun.*, vol. 12, no. 12, pp. 5992–6010, Dec. 2013.
[23] A. Sabharwal, P. Schniter, D. Guo, D. W. Bliss, S. Rangarajan, and R. Wichman, "In-band full-duplex wireless: Challenges and opportunities," *IEEE J. Sel. Areas Commun.*, vol. 32, no. 9, pp. 1637–1652, Sep. 2014.
[24] *System Scenarios and Technical Requirements for Full-Duplex Concept*, accessed on Apr. 30, 2013. [Online]. Available: http://www.fp7-duplo.eu/index.php/deliverables
[25] S. Huberman and T. Le-Ngoc, "MIMO full-duplex precoding: A joint beamforming and self-interference cancellation structure," *IEEE Trans. Wireless Commun.*, vol. 14, no. 4, pp. 2205–2217, Apr. 2015.
[26] D. Nguyen, L.-N. Tran, P. Pirinen, and M. Latva-Aho, "On the spectral efficiency of full-duplex small cell wireless systems," *IEEE Trans. Wireless Commun.*, vol. 13, no. 9, pp. 4896–4910, Sep. 2014.
[27] H. H. Kha, H. D. Tuan, and H. H. Nguyen, "Fast global optimal power allocation in wireless networks by local D.C. programming," *IEEE Trans. Wireless Commun.*, vol. 11, no. 2, pp. 510–515, Feb. 2012.
[28] H. Tuy, *Convex Analysis and Global Optimization*. Norwell, MA, USA: Kluwer, 1998.
[29] B. P. Day, A. R. Margetts, D. W. Bliss, and P. Schniter, "Full-duplex bidirectional MIMO: Achievable rates under limited dynamic range," *IEEE Trans. Signal Process.*, vol. 60, no. 7, pp. 3702–3713, Jul. 2012.
[30] D. Tse and P. Viswanath, *Fundamentals of Wireless Communication*. New York, NY, USA: Cambridge Univ. Press, 2005.
[31] D. Katselis, E. Kofidis, and S. Theodoridis, "On training optimization for estimation of correlated MIMO channels in the presence of multiuser interference," *IEEE Trans. Signal Process.*, vol. 56, no. 10, pp. 4892–4904, Oct. 2008.
[32] Y. S. Cho, J. Kim, W. Y. Yang, and C. G. Kang, *MIMO-OFDM Wireless Communications With MATLAB*. Hoboken, NJ, USA: Wiley, 2010.
[33] Q. Shi, W. Xu, J. Wu, E. Song, and Y. Wang, "Secure beamforming for MIMO broadcasting with wireless information and power transfer," *IEEE Trans. Wireless Commun.*, vol. 14, no. 5, pp. 2841–2853, May 2015.
[34] M. Mohammadi, H. A. Suraweera, Y. Cao, I. Krikidis, and C. Tellambura, "Full-duplex radio for uplink/downlink wireless access with spatially random nodes," *IEEE Trans. Commun.*, vol. 63, no. 12, pp. 5250–5266, Dec. 2015.
[35] M. Grant and S. Boyd. (Mar. 2014). *CVX: MATLAB Software for Disciplined Convex Programming, Version 2.1*. [Online]. Available: http://cvxr.com/cvx

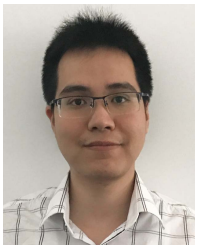

Ho Huu Minh Tam was born in Ho Chi Minh City, Vietnam. He received the B.S. degree in electrical engineering and telecommunications from the Ho Chi Minh City University of Technology, in 2012. He is currently pursuing the Ph.D. degree with the University of Technology Sydney, Sydney, NSW, Australia, under the supervision of Prof. H. D. Tuan. His research interests include optimization techniques in signal processing for wireless communications.

Hoang Duong Tuan received the Diploma (Hons.) and Ph.D. degrees in applied mathematics from Odessa State University, Ukraine, in 1987 and 1991, respectively. He spent nine academic years as an Assistant Professor with the Department of Electronic-Mechanical Engineering, Nagoya University, Japan, from 1994 to 1999, and then as an Associate Professor with the Department of Electrical and Computer Engineering, Toyota Technological Institute, Nagoya, from 1999 to 2003. He was a Professor with the School of Electrical Engineering and Telecommunications, The University of New South Wales, from 2003 to 2011. He is currently a Professor with the Faculty of Engineering and Information Technology, University of Technology Sydney. His research interests include optimization, control, signal processing, wireless communication, and biomedical engineering for over 20 years.

Ali Arshad Nasir (S'09–M'13) received the Ph.D. degree in telecommunications engineering from Australian National University, Australia, in 2013. He was a Research Fellow from 2012 to 2015. He was an Assistant Professor with the School of Electrical Engineering and Computer Science, National University of Sciences and Technology, Pakistan, from 2015 to 2016. He is an Assistant Professor with the Department of Electrical Engineering, King Fahd University of Petroleum and Minerals, Dhahran, Saudi Arabia. His research interests include signal processing in wireless communication systems. He is an Associate Editor of the IEEE CANADIAN JOURNAL OF ELECTRICAL AND COMPUTER ENGINEERING.

Trung Q. Duong (S'05–M'12–SM'13) received the Ph.D. degree in telecommunications systems from the Blekinge Institute of Technology, Sweden, in 2012. Since 2013, he has been with Queen's University Belfast, Belfast, U.K., as a Lecturer (Assistant Professor). His current research interests include small-cell networks, physical layer security, energy-harvesting communications, and cognitive relay networks. He is the author or co-author of 240 technical papers published in scientific journals (125 articles) and he has presented at international conferences (115 papers).

Dr. Duong was awarded the Best Paper Award at the IEEE Vehicular Technology Conference (VTC-Spring) in 2013, the IEEE International Conference on Communications (ICC) 2014, and the IEEE Global Communications Conference (GLOBECOM) 2016. He is a recipient of the prestigious Royal Academy of Engineering Research Fellowship (2016–2021). He currently serves as an Editor of the IEEE TRANSACTIONS ON WIRELESS COMMUNICATIONS, the IEEE TRANSACTIONS ON COMMUNICATIONS, and *IET Communications*, and a Senior Editor of the IEEE COMMUNICATIONS LETTERS.

H. Vincent Poor (S'72–M'77–SM'82–F'87) received the Ph.D. degree in EECS from Princeton University in 1977. From 1977 until 1990, he was on the faculty of the University of Illinois at Urbana–Champaign. Since 1990, he has been on the faculty at Princeton, where he is currently the Michael Henry Strater University Professor of Electrical Engineering. From 2006 to 2016, he served as the Dean of Princeton's School of Engineering and Applied Science. His research interests are in the areas of information theory, statistical signal processing and stochastic analysis, and their applications in wireless networks and related fields, such as smart grid and social networks. Among his publications in these areas is the book *Mechanisms and Games for Dynamic Spectrum Allocation* (Cambridge University Press, 2014).

Dr. Poor is a member of the National Academy of Engineering and the National Academy of Sciences, and is a foreign member of the Royal Society. He is also a fellow of the American Academy of Arts and Sciences, the National Academy of Inventors, and other national and international academies. He received the Marconi and Armstrong Awards of the IEEE Communications Society in 2007 and 2009, respectively. Recent recognition of his work includes the 2016 John Fritz Medal, the 2017 IEEE Alexander Graham Bell Medal, honorary professorships at Peking University and Tsinghua University, both conferred in 2016, and a D.Sc. *honoris causa* from Syracuse University in 2017.